

AN ABSTRACT OF THE THESIS OF

Brandy J. Saffell for the degree of Master of Science in Forest Ecosystems and Society presented on June 11, 2013.

Title: Impacts of Swiss Needle Cast on Douglas-fir Tree-ring Stable Isotopes and Tree Carbohydrate Reserves.

Abstract approved:

Frederick C. Meinzer

Understanding the mechanisms of disease in forest pathology is a critical component to learning how to most efficiently manage tree diseases like Swiss needle cast (SNC). SNC is an economically important, fungal disease of Douglas-fir (*Pseudotsuga menziesii* [Mirb.] Franco) that is prevalent in coastal areas of the Pacific Northwest. This thesis research provides two contributions to the greater understanding of the pathogenic impacts on plant physiological functioning, or *pathophysiology*, of SNC on Douglas-fir that will ultimately inform management decisions in Pacific Northwest forests affected by SNC. The primary objectives of this thesis research were: (1) to examine the effects of SNC on Douglas-fir tree-ring stable isotope discrimination of carbon ($\Delta^{13}\text{C}$) and oxygen ($\delta^{18}\text{O}$) and (2) to evaluate the impact of SNC on tree carbohydrate reserves.

Thesis Objective 1- I used growth measurements and stable isotopes of carbon and oxygen in tree-rings of Douglas-fir and a non-susceptible reference species (western hemlock, *Tsuga heterophylla* (Raf.) Sarg.) to evaluate their use as proxies for

variation in past SNC infection, particularly in relation to potential explanatory climate factors. Trees were sampled from a site where a fungicide trial took place from 1996 to 2000, which enabled the comparison of years when disease was present and absent, relative to untreated trees which had the infection throughout. Tree-ring $\Delta^{13}\text{C}$ of treated Douglas-fir increased during the treatment period, and was $\sim 1.6\text{ ‰}$ greater than that of untreated Douglas-fir at the end of the years of the fungicide treatment. Both annual growth and tree-ring $\Delta^{13}\text{C}$ increased with treatment such that treated Douglas-fir had values similar to co-occurring western hemlock during the treatment period, which suggests that the use of $\Delta^{13}\text{C}$ in Douglas-fir tree-rings to track SNC disease history may be a practical approach provided a reference species is available to develop a parallel $\Delta^{13}\text{C}$ chronology. There was no difference in tree-ring $\delta^{18}\text{O}$ between treated and untreated Douglas-fir. Tree-ring $\Delta^{13}\text{C}$ of diseased Douglas-fir was negatively correlated with relative humidity (RH) during the two previous summers, consistent with increased leaf colonization by SNC under high humidity conditions that then lead to greater disease severity in following years.

Thesis Objective 2- The effects of SNC on Douglas-fir carbohydrate reserves were explored to evaluate the extent to which non-structural carbohydrate (NSC) can be mobilized under natural conditions of low water stress and restricted carbon supply in relation to potential demands for growth. Concentrations of starch, sucrose, glucose and fructose were analyzed in twig wood, foliage, and trunk sapwood of 15 Douglas-fir trees expressing a gradient of SNC symptom severity. There were significant

negative relationships between disease severity and growth (mean basal area increment, BAI), as well as between disease severity and mean concentration of trunk NSC. The amount of NSC per unit growth (mean NSC/BAI), an index of the relative priority of storage versus growth, increased with disease severity in all three sampled tissues. These results suggest that under reduced carbon supply with SNC, Douglas-fir trees retain NSC at the expense of growth. The crown retains the most NSC, presumably to maintain foliage growth in the spring to compensate for SNC-induced rapid foliage loss in the summer and fall.

© Copyright by Brandy J. Saffell
June 11, 2013
All Rights Reserved

Impacts of Swiss Needle Cast on Douglas-fir Tree-ring Stable Isotopes and Tree
Carbohydrate Reserves

by
Brandy J. Saffell

A THESIS

submitted to

Oregon State University

in partial fulfillment of
the requirements for the
degree of

Master of Science

Presented June 11, 2013
Commencement June 2014

Master of Science thesis of Brandy J. Saffell presented on June 11, 2013.

APPROVED:

Major Professor, representing Forest Ecosystems and Society

Head of the Department of Forest Ecosystems and Society

Dean of the Graduate School

I understand that my thesis will become part of the permanent collection of Oregon State University libraries. My signature below authorizes release of my thesis to any reader upon request.

Brandy J. Saffell, Author

ACKNOWLEDGMENTS

I would like to express my sincere appreciation to many people for their support and guidance throughout my graduate program. First and foremost, I would like to thank my brilliant advisor, Dr. Rick Meinzer, for his encouragement and advocacy, and for the invaluable opportunity to study tree physiology under his guidance. I am indebted to my circle of scientific support, Drs. Steve Voelker, Dave Shaw, Dave Woodruff, Renée Brooks, Barb Lachenbruch and Kate McCulloh, for providing helpful advice and ideas that have shaped my thesis and made me an immensely stronger scientist and critical thinker. Also, thank you to my GCR, Dr. Ryan Contreras.

A very special thank you to the Swiss Needle Cast Cooperative and the National Science Foundation for their enthusiasm and generous financial support that made this research possible. Thank you to my fellow graduate students, Danielle Marias and Kelly Kerr, and all of my field and lab helpers, Kristen Falk, Joshua Petitmermet, Ben Roberts-Pierel, Regina Kurapova, Alena Tofte, Valerie Simms, and Holly Kearns, for making research fun.

Finally, I cannot be grateful enough to my friends and family, whose love carried me through this degree program: Lynda Saffell and Mel Ferganbaum, Brian and Terry Saffell, Billy Saffell, Jannette Saffell, Lynn and Bill Smalley, Karina Martins, Tyan Long, Anna Horn, Vida Pedersen, and Jordan Weinstein. Thank you to my knitting circle, for listening. Thank you to my housemates, for taking me dancing. And thank you to my partner, Joshua Weinstein, for being my everything. This thesis is dedicated to you all.

CONTRIBUTION OF AUTHORS

Chapter 2: Drs. Frederick C. Meinzer and Steve L. Voelker were instrumental in the study design, interpretation, and manuscript editing; Dr. David C. Shaw assisted in manuscript editing and provided his expertise in forest pathology; Dr. J. Renée Brooks assisted in interpretation and manuscript editing, and provided her expertise in stable isotopes in plant ecology; Dr. Barbara Lachenbruch assisted in the study design and manuscript editing, and provided her expertise in tree physiology; Dr. Jennifer McKay was responsible for carbon stable isotope measurement, and provided her expertise in stable isotope theory.

Chapter 3: Drs. Frederick C. Meinzer and David R. Woodruff were invaluable in the study design, sampling, interpretation, and manuscript editing; Dr. David C. Shaw was instrumental in site selection and manuscript editing, and provided his expertise in forest pathology; Dr. Steve L. Voelker assisted in manuscript editing and provided his expertise in tree physiology; Dr. Barbara Lachenbruch assisted in manuscript editing and provided her expertise in tree physiology; Kristen Falk was incredibly helpful in non-structural carbohydrate sample collection, preparation, and assays.

TABLE OF CONTENTS

	<u>Page</u>
Chapter 1 – Introduction	1
Background - Fungal foliage diseases of North American trees.....	2
Pathophysiology of SNC on Douglas-fir	6
Fungus life cycle	6
Needle and canopy processes.....	7
Tree growth	9
Wood properties	9
Ecological considerations.....	11
Climate	13
Thesis research objectives.....	14
Chapter 2 – Tree-ring stable isotopes record the impact of a foliar fungal pathogen on CO ₂ assimilation and growth in Douglas-fir	15
Abstract	15
Introduction	16
Materials and methods	19
Carbon stable isotope conceptual approach	19
Oxygen stable isotope conceptual approach	22
Field site and sampling.....	26
Annual growth analysis.....	27
Stable isotope analyses.....	27
Climate data.....	29

TABLE OF CONTENTS (Continued)

	<u>Page</u>
Statistical analyses.....	30
Results	31
Annual growth.....	31
Branch carbon stable isotopes	31
Tree-ring carbon stable isotopes	32
Tree-ring oxygen stable isotopes.....	33
Climate analyses.....	33
Discussion	34
Annual growth and carbon stable isotopes.....	35
Oxygen stable isotopes.....	39
Disease severity and climate	41
Acknowledgements	43
Chapter 3 – Seasonal carbohydrate dynamics and growth in Douglas-fir trees experiencing chronic, fungal-mediated reduction in functional leaf area.....	52
Abstract	52
Introduction	52
Materials and methods	57
Field site and sampling.....	57
Disease severity assessment.....	59
Chemical analyses	60
Growth analyses	61

TABLE OF CONTENTS (Continued)

	<u>Page</u>
Statistical analyses.....	62
Results	62
Disease severity assessment.....	62
NSC and growth analyses	63
Discussion	66
Acknowledgements	73
Chapter 4 – Thesis Summary	82
Bibliography.....	85
Appendix	99
Appendix A- Chapter 3 Supporting Information	100

LIST OF FIGURES

<u>Figure</u>	<u>Page</u>
2.1 Mean basal area increment (BAI) of fungicide-treated and untreated Douglas-firs at the Beaver, Oregon site during the years of observation (1989-2011; n=6 trees per treatment).....	45
2.2 $\Delta^{13}\text{C}$ of foliage and twig wood samples from branch cohorts aged 0 to 3 years old at the Prairie Hill site (n=6 trees).	46
2.3 Mean $\Delta^{13}\text{C}_{\text{cell}}$ of western hemlock (a), and fungicide-treated and untreated Douglas-firs (b) at the Beaver, Oregon site during the years of observation (1989-2011; n=6 trees per treatment)	47
2.4 Scatterplot of mean tree-ring $\Delta^{13}\text{C}_{\text{cell}}$ and mean basal area increment (BAI) of fungicide-treated Douglas-fir post-, during, and pre-treatment (n=6 trees per treatment).....	48
2.5 Mean tree-ring $\delta^{18}\text{O}_{\text{cell}}$ of western hemlock (a), and fungicide-treated and untreated Douglas-firs (b) at the Beaver, Oregon site during the years of observation (1989-2011; n=6 trees per treatment)	49
2.6 Pearson correlation coefficients (r) of Douglas-fir and western hemlock tree-ring $\Delta^{13}\text{C}_{\text{cell}}$ and various climate variables at different times of year (previous-year monthly values, previous growing season average (May-July, GS), previous summer average (June-September; Smr), and two-years-previous summer average (Smr ⁻²))	50
2.7 Modeled relationship between stomatal conductance (g_s) and the resulting difference in $\Delta^{18}\text{O}_{\text{cell}}$ from a control ($g_s = 0.14 \text{ mol m}^{-2} \text{ s}^{-1}$) following equations 3-6.....	51
3.1 Mean foliage mass per branch growth increment for each sampled foliage tissue age at each sampling date (bars represent one standard error).....	76
3.2 Mean annual 2000-2011 BAI versus functional foliage mass with each point representing one tree and simple linear regression analysis.....	77
3.3 Mean non-structural carbohydrate (NSC) content for current year foliage and twigs, and trunk tissue, for each sampling date, and mean 2000-2011 basal area increment (BAI) for each sampled tree.....	78

LIST OF FIGURES (Continued)

<u>Figure</u>	<u>Page</u>
3.4 Mean trunk non-structural carbohydrate (NSC) content (a) and mean trunk NSC/ basal area increment (BAI) (b) versus functional foliage mass.....	79
3.5 Mean twig (a) and foliage (b) non-structural carbohydrate (NSC) content and mean twig (c) and foliage (d) NSC/basal area increment (BAI) versus functional foliage mass.....	80
3.6 Mean foliage, twig, and trunk non-structural carbohydrate (NSC) concentrations for current year foliage and twigs, and trunk tissue, for each sampling date (ordered June, July, and September for each tree)	81

LIST OF TABLES

<u>Table</u>	<u>Page</u>
2.1 Characteristics of each treatment group (n=6 for each group), including age (determined from cores), diameter at breast height (DBH), height, and crown width (diameter) with one standard deviation from the mean in parentheses.....	44
3.1 Individual characteristics for the sampled trees in ascending order by basal area increment (BAI).....	74
3.2 Mean concentrations (% dry weight) of total non-structural carbohydrate (NSC), starch, sucrose, and glucose and fructose (Gluc/Fruc) of the trunk, and current-year twigs and foliage of the sampled trees from each sampling date.....	75

LIST OF APPENDIX TABLES

<u>Table</u>	<u>Page</u>
A.1 Average total non-structural carbohydrate, starch, sucrose, and glucose and fructose concentrations (% dry weight) of twigs and foliage from 2011, 2010, and 2009 cohorts of Douglas-fir trees with Swiss Needle Cast sampled in mid-June.	100
A.2 Average total non-structural carbohydrate, starch, sucrose, and glucose and fructose concentrations (% dry weight) of twigs and foliage from 2011, 2010, and 2009 cohorts of Douglas-fir trees with Swiss Needle Cast sampled in late July.	101
A.3 Average total non-structural carbohydrate, starch, sucrose, and glucose and fructose concentrations (% dry weight) of twigs and foliage from 2011, 2010, and 2009 cohorts of Douglas-fir trees with Swiss Needle Cast sampled in early September.	102

Impacts of Swiss Needle Cast on Douglas-fir Tree-ring Stable Isotopes and Tree Carbohydrate Reserves

Chapter 1

Introduction

Swiss needle cast (SNC), the foliage disease caused by the fungus *Phaeocryptopus gaeumannii* (T. Rohde) Petr., has negatively affected the productivity of Douglas-fir (*Pseudotsuga menziesii* (Mirb.) Franco) forests in the Pacific Northwest for over 25 years. Douglas-fir stands with SNC can experience growth losses ranging from 23-52% in cubic volume, dependent upon the degree of disease severity (Maguire *et al.*, 2002). Possibly the most alarming aspect of the disease is its vast spatial extent and the apparent lack of progress in its control. Since the first SNC aerial survey of the Oregon coast in 1996, the total area affected has increased from about 53,000 ha, the lowest recorded value to date, to about 180,000 ha in 2011 (Kanaskie & McWilliams, 2010; A. Kanaskie, pers. comm.).

P. gaeumannii was present in the Pacific Northwest before SNC was ever an important disease. The first record of the fungus and SNC appears in the mid-1920s after a severe SNC epidemic of U.S.-imported Douglas-fir in Switzerland (Boyce, 1940). It was not until the late 1980s that the fungus began causing significant needle loss and growth reductions to Douglas-fir in the Pacific Northwest. Due to the sudden manifestation of SNC and the clear economic losses that it has caused, there has been a significant amount of research focused on the disease.

Several SNC studies have concentrated on the quantification and elucidation of pathogenic impacts on Douglas-fir physiological functioning, or the pathophysiology of the disease. Pathophysiology is a comparatively young field of research that has immense potential to aid scientists and foresters alike in better understanding the mechanisms of diseases to ultimately learn how to better manage them. The purpose of this introduction is to (1) synthesize information on fungal foliage diseases of trees in North America, (2) review past research on the effects of SNC on Douglas-fir biology and physiology, as well as the relationship between SNC and climate, and (3) to describe the objectives of this thesis research and its potential contributions to the greater understanding of the pathophysiology of Swiss Needle Cast on Douglas-fir.

Background- Fungal foliage diseases of North American trees

Ascomycetes are the primary pathogens of tree foliage diseases. Oomycetes and basidiomycetes are also known to cause leaf damage, but because their damage to leaves is secondary to more destructive manifestations of disease on other plant parts (e.g. stem cankers from the oomycete *Phytophthora ramorum* Werres, or root rot from the basidiomycete *Phellinus weirii* (Murrill) Gilb.), they will not be included in this discussion. The cycle of infection is nearly universal for fungal foliage pathogens and is tied strongly to the seasons and climate (Manion, 1991; Agrios, 2005). Sexual spores are released in spring at tree bud burst and land on the leaf surface. Moisture is the limiting factor during spring colonization because spores are dependent upon leaf wetness to release both sexual and asexual spores and to germinate (Edmonds *et al.*,

2011). During germination, the hyphae may either directly penetrate the cuticle or enter the leaf through the stomata. Once inside the leaf, the mycelia typically produce haustoria, which are specialized appendages for nutrient absorption that can obtain nutrition by: (1) absorbing nutrients through the plant cell wall, (2) penetrating the cell wall, enclosing the cell plasma membrane, and then absorbing cell nutrients, or (3) penetrating through the cell wall and plasma membrane (Honegger, 1986). Some fungi are simply epiphytic and do not kill cells in the leaf. Throughout the summer, asexual reproductive structures (*i.e.* conidia) release large loads of spores and increase the amount of infected foliage. The mycelia over-winter inside of living leaves or in dead foliage on the forest floor, until the following spring when sexual fruiting bodies emerge and the cycle begins again.

Symptoms of disease vary with the particular causal pathogen. Generally, there can be necrotic spots or whole necrotic leaves, fruiting bodies in necrotic areas, shriveled foliage, and needle chlorosis (Sinclair & Lyon, 2005). Necrotic spots are usually dry and strictly delimited, occasionally falling out in the center (*i.e.* shot holes). In conifers, foliar pathogens can often lead to sparse crown coverage due to premature defoliation (Manion, 1991). Angiosperms may also be defoliated but can produce a second crop of leaves in some cases.

There are several examples of foliage diseases of North American hardwoods. *Septoria* leaf spot and canker (caused by *Septoria* spp.) infects cottonwood and hybrid poplar, especially when the trees are grown in intense culture (Manion, 1991). The cankerous spots can be either circular in a bull's-eye formation or irregularly spaced,

and tree growth loss is directly proportional to disease intensity. Powdery mildew is a common disease associated with many plants that causes a white cast on the leaves due to the hyphae of the fungus growing on the outer surface (Agrios, 2005; Glawe, 2008). Genera of fungi causing powdery mildew include *Sphaerotheca* Lév., *Erysiphe* D.C., *Podosphaera* Kunze, *Microsphaera* Lév., *Uncinula*, and *Phyllactinia* Lév. Anthracnose is an artificial grouping of different foliage diseases that cause similar symptoms (e.g. *Kabatella apocrypta* (Ellis & Everh.) in *Acer* spp. L.; and *Apiognomonina* spp. Höhn. in *Quercus* spp. L., *Fraxinus* spp. L., and *Platanus* spp. L.). Infected leaves develop irregular dead blotches that gradually merge to kill the whole leaf and occasionally infect the twig (Manion, 1991; Edmonds *et al.*, 2011).

Foliage diseases in North American conifers are especially important because the trees cannot re-foliate until the year following substantial foliar damage or defoliation, resulting in severe growth reduction or mortality (Hansen & Lewis, 1997). There are several conifer diseases that cause needle necrosis or blistering, and subsequent abscission, although the exact underlying process of host tissue death and specific characteristics of symptoms may differ between pathogen species. These diseases include, but are not limited to: Dothistroma blight (caused by *Dothistroma septosporum*) that affects over 70 species of pines, Rhabdocline needle cast (caused by *Rhabdocline* spp. Syd.) of Scots pine (*Pinus sylvestris* L.) and Douglas-fir, brown spot needle blight (caused by *Mycosphaerella dearnessii* M.E. Barr) of longleaf and other pines (*Pinus palustris* Mill.), and Elytroderma needle cast (caused by *Elytroderma deformans* (Weir) Darker) of various pine host species. In addition, snow molds, also

called brown felt blights (caused by *Herpotrichia* spp. Fuckel), cover needles with thick, dark hyphae and plug stomata (Tainter & Baker, 1996).

In general, ascomycetous fungi that cause foliage diseases are parasitic and extract or divert nutrients from their host through structural or biochemical mechanisms (Manter *et al.*, 2000; Agrios, 2005). Structural mechanisms of disease indirectly affect host processes, for example, by destroying host leaf tissue or physically blocking intercellular spaces and stomata. Dothistroma blight releases a toxin (dothistromin) within host needles that causes structural host damage by killing cells in advance of mycelial growth (Brown *et al.*, 2003). The destruction of host tissue decreases the amount of light-absorbing chlorophyll, damages the photosynthetic machinery in the thylakoid membrane, and generally reduces the ability of the needle to assimilate carbon. Snow molds also structurally cause disease by blocking light from entering the leaf and clogging stomata with hyphae (Simms, 1967), which can affect photosynthetic rate, concentration of CO₂ inside the leaf, and overall carbohydrate synthesis. Biochemical mechanisms of disease are not completely understood in trees, but there has been some research on fungal foliage diseases that directly affect leaf processes in smaller plants. For example, Gordon and Duniway (1982) found that the presence of a powdery mildew (*E. polygoni* D.C.) on sugar beet (*Beta vulgaris* L.) was responsible for reductions in the maximum photosynthetic rate, mesophyll conductance, and rubulose-1,5-bisphosphate carboxylase oxygenase (rubisco) activity.

Pathophysiology of SNC on Douglas-fir

SNC primarily operates using a structural mechanism of disease with biochemical implications, and does not kill plant cells directly. The lifecycle of *P. gaeumannii* interferes with normal Douglas-fir physiological functioning during key phases of the host's lifecycle. The first symptoms of disease are evident in the needles and tree canopy. As disease severity increases over time, other plant structures and processes show symptoms of disease. These changes in tree structure and function have significant implications for Douglas-fir ecological relationships.

Fungus life cycle

SNC is a monocyclic disease with a fungal life cycle that has been observed and described in several publications (Rhode, 1937; Boyce, 1940; Ford & Morton, 1971; Chen, 1972; Hood & Kershaw, 1975; Hood, 1982; Chastagner & Byther, 1983; Michaels & Chastagner, 1984). Asci begin to emerge and sporulate in May and June in coordination with Douglas-fir bud break. Ascospores are released throughout spring and summer months and only infect new, current year foliage (Hansen *et al.*, 2000). Fungal hyphae colonize the surface of the needle and move inside the leaf via the stomata (Chen, 1972). Hyphal growth continues until mycelia are tightly packed within the leaf intercellular space. In the worst cases of infection, the fungal fruiting bodies, or pseudothecia, emerge through the stomata during the spring months of the year following infection, at which point spores are released and the cycle begins again. Needle chlorosis and foliage loss increase with high disease pressure (or spore load)

and needle age as the fungus can produce more pseudothecia over several years (Hansen *et al.*, 2000). In the most severe cases, current year needles are the only remaining foliage for the majority of the growing season (Manter *et al.*, 2003a).

Needle and canopy processes

The emergence of pseudothecia from needle stomata is the structural mechanism of disease (Manter *et al.*, 2000). The impact of the disease does not become evident for approximately 10 months, usually April in the year following infection. At this point, there is a strong linear relationship between the fraction of stomata occluded by pseudothecia and the percent decline in stomatal conductance. As the spring progresses and more pseudothecia block the stomata, stomatal conductance continues to decrease each month. In a greenhouse experiment on *P. gaeumannii*-inoculated Douglas-fir seedlings, Manter *et al.* (2000) found that stomatal conductance of Douglas-fir with SNC was approximately 36%, 38%, and 83% less in April, May, and June, respectively, compared to a control. When stomatal conductance decreases in infected needles, compensatory increases in conductance do not occur in less infected needles or unblocked stomata (Manter & Kavanagh, 2003).

It is well known that reductions in stomatal conductance can limit photosynthesis because stomatal pore size governs the amount of CO₂ that can enter the leaf per unit time. The pseudothecia-blocked stomata restrict the entrance of CO₂ into the leaf, and thus decrease the availability of CO₂ for carbon assimilation. Manter *et al.* (2000) found that the net carbon assimilation rate of Douglas-fir with SNC was

approximately 56%, 62%, and 72% less in April, May, and June, respectively, compared to a control. The same study also found that the amount of activated rubisco decreased with increasing occluded stomata. Rubisco requires a molecule of CO₂ for activation, so the decrease in CO₂ concentration within the leaf likely caused this result.

Another mode of photosynthetic inhibition mediated by the fungus could result from the mat of hyphae growing across the needle surface, which would restrict the amount of incoming light and diffusion of CO₂ (Manter *et al.*, 2000). The fungus does not produce haustoria, penetrate the cells of the inner leaf, or cause necrosis, and thus it is not clear how and to what extent the fungus obtains photosynthate from its host (Capitano, 1999; Stone *et al.*, 2008a).

A number of studies have focused on the cause of needle abscission and the implications of a reduction in carbon supply on the tree carbon budget. A study by Manter *et al.* (2003a) found that once about 25% of stomata were occluded, the leaf ceased to be a carbon source and became a carbon sink. This means that although the leaves still photosynthesized during daylight hours, the respiration costs to maintain leaf functionality yielded a negative total carbon balance. The authors also found that once a leaf became a carbon sink, it usually was abscised. Another factor that may contribute to needle loss is the effect of disease on energy dissipation and photoinhibition. Manter (2002) reported that excess absorbed light at high photosynthetically active photon flux densities (PPFD) was twice as high in infected needles as in uninfected needles. The same study also found that after a one hour

high light treatment, the decline in the efficiency of photosystem II (PSII) was 1.5 times greater in infected needles than control needles, and the increase in minimum fluorescence was greater in infected needles (~178%) than control needles (~122%). All together, these results suggest that the greater decline in PSII efficiency of infected needles could largely be due to photo-oxidative damage, which could contribute to needle abscission. As needle retention decreases, the net photosynthetic rate for the entire plant decreases linearly (Manter *et al.*, 2003a). Surprisingly, trees growing in severely diseased stands still maintain a positive carbon budget for the year. Loss of foliage from previous years causes diseased trees to rely on their current-year needles as the main source of photosynthate.

Tree growth

With increasing disease severity and subsequent needle loss, trees with SNC do not grow as well as healthy trees. Maguire *et al.* (2002) found an inferred average volume growth loss of 23% over 75,700 ha of Douglas-fir plantations with SNC in a single year, but growth loss could be as great as 52% in the most severely diseased stands. Mainwaring *et al.* (2005) and Maguire *et al.* (2011) found a similar decline in tree basal area and volume. Moreover, another study using tree-rings reported that stands with SNC had reduced growth by as much as 85% since 1984 compared to a control (Black *et al.*, 2010).

Wood properties

In agreement with the studies discussed in the previous section, Johnson *et al.* (2003) found that the latewood and earlywood growth in tree-rings of Douglas-fir with SNC was significantly less than that of nearby trees sprayed with a fungicide treatment for several consecutive years (44 and 68% less growth in latewood and earlywood, respectively). The untreated trees (with SNC) had a 10.6% higher latewood proportion than treated trees, as well as earlywood with thinner cell walls (3.18 and 5.35 μm for untreated and treated trees, respectively). Earlywood is known to form in early spring before bud break, accordingly relying on photosynthate from older foliage cohorts (Onaka, 1950). The untreated trees had less foliage before bud break than the treated trees, and therefore, they had a smaller earlywood to latewood ratio and earlywood with less structural integrity, or thinner cell walls.

Furthermore, untreated trees exhibited a smaller sapwood area, lower sapwood moisture content, and more gas-filled space in the sapwood. The authors speculated that the lower sapwood moisture content in untreated trees could be associated with a decrease in sap flow and specific conductivity (Puritch, 1971; Edwards & Jarvis, 1982; Granier *et al.*, 2000). Furthermore, the authors showed that the lower moisture content and higher gas content of diseased trees was more than the amount accounted for by the increased proportion of latewood. The most logical explanation for the increased gas and decreased moisture content of sapwood from diseased trees was that there was more native embolism in the diseased trees. They speculated that this increased embolism could have resulted from a SNC-induced reduction in available

photosynthate that in healthier trees would be used to reverse sapwood embolism (Holbrook & Zwieniecki, 1999).

A further study examined 15 stands of Douglas-fir to learn the effects of SNC disease severity on wood properties at both the stand and within-stand levels (Johnson *et al.*, 2005). Like Johnson *et al.* (2003), they found that trees from stands with less than two years of needle retention had higher wood density and lower sapwood moisture content than trees from healthier stands with higher needle retention. In addition, trees with more severe disease symptoms had higher modulus of elasticity (MOE) and latewood proportion than trees from healthier stands. The authors concluded that the increase in latewood proportion of trees with more severe disease symptoms could potentially be the cause of increased stiffness (MOE).

Ecological considerations

Kelsey and Manter (2004) found that trees in stands with moderate SNC had lowered wound-induced oleoresin flow, as well as less ethanol and monoterpene production, compared to trees in Douglas-fir stands with low SNC. The authors ascribed these results to reduced availability of photosynthate since carbohydrates are an important building block of defense compounds (Harry & Kimmerer, 1991; Kelsey & Joseph, 1998). In the same study, Douglas-fir beetles (*Dendroctonus pseudotsugae* Hopkins) were found to be more attracted to stands of Douglas-fir with low SNC than a nearby stand with moderate SNC. Because it has been suggested that bark beetles are attracted to a host tree by certain chemical compounds, including ethanol, it is possible

that comparatively low ethanol concentrations in the phloem of moderately diseased trees renders them less attractive to bark beetles than trees with low disease (Pitman *et al.*, 1975; Ross & Daterman, 1997). However, moderately diseased stands had deeper and more numerous beetle galleries and deeper sapwood penetration than stands with low disease. These results suggest that although beetles were more attracted to stands with low disease, potentially due to comparatively higher ethanol concentrations, they caused more damage to moderately diseased stands due to impaired tree defenses.

The significant loss of carbohydrates from roots below ground, accounting for an estimated 73% of net primary productivity in coniferous temperate forests (Grier *et al.*, 1981; Fogel & Hunt, 1983), should also be affected by reduced carbon supply due to SNC. There is evidence that a reduction in carbon supply from the crown (*e.g.* from defoliation) can lead to depleted NSC reserves in roots of conifers (Webb & Karchesy, 1977; Oleksyn *et al.*, 2000). Reduced NSC export might limit root exudation, which plays a vital role in cycling of soil organic matter (Millard *et al.*, 2007) and attracting and establishing symbiotic relationships with mycorrhizae (*e.g.* Graham, 1982), which have been shown to receive approximately 30% of total assimilate from the host tree (reviewed by Soderström, 2002). Luoma and Eberhart (2006) observed that SNC-diseased Douglas-fir stands had a lower density and diversity of ectomycorrhizal fungi than the density and diversity that were typically found in healthy stands, suggesting that the reduction in photosynthate associated with SNC could have profound effects on below-ground processes.

Climate

An important part of understanding a disease epidemic such as SNC in Oregon is identifying the environment that the pathogen requires to develop and reproduce. The clearest geographic pattern of the disease is that SNC appears to increase in severity with proximity to the coast (Rosso & Hansen, 2003; Zhao *et al.*, 2011). The landscape-sized scale of the disease symptoms suggests that coastal climatic factors interact with the strong seasonality of the fungus' life cycle. Generally, warm ambient temperatures in winter and cool summers seem to encourage hyphal growth and development of reproductive structures (Rosso & Hansen, 2003; Manter *et al.*, 2005; Coop & Stone, 2007; Stone *et al.*, 2008b; Latta *et al.*, 2009). Large differences between the coldest and hottest day of the year appear to limit fungal abundance (Zhao *et al.*, 2011). It is also clear that increased leaf wetness in spring and summer is associated with disease severity (Rosso & Hansen, 2003; Manter *et al.*, 2005; Coop & Stone, 2007; Latta *et al.*, 2009), possibly because leaf wetness facilitates fungal spore establishment and germination (Capitano, 1999). Although previous research has identified the aforementioned climatic variables as helpful in predicting fungal abundance and needle retention, results from these studies report much unexplained spatial variation of the two factors and tend to conflict over which climate variables are most important. The discrepancies between these study results could likely be due to their differing methods of SNC quantification (*i.e.* fungal abundance versus needle retention), both of which approximate the actual effect of SNC on tree health.

Thesis research objectives

In this thesis research, I will examine two aspects of the impact of SNC on Douglas-fir physiology.

Objective 1: I propose to examine the effects of SNC on Douglas-fir tree-ring stable isotopes of carbon and oxygen. If there is a distinguishable difference in stable isotope ratios of tree-rings in the presence and absence of disease, stable isotopes of tree-rings could be a useful tool in examining the past occurrence of SNC on the Oregon coast. In addition, this study could provide insight into leaf processes that are modified by the presence of *P. gaeumannii* in Douglas-fir foliage since stable isotopes reflect leaf physiological processes. Furthermore, if stable isotopes in tree-rings serve as an adequate proxy of past disease variation, they could be used in conjunction with records of past climate factors (*e.g.* precipitation and temperature) to identify environmental conditions associated with variations in disease severity.

Objective 2: I propose to evaluate the impact of SNC on tree carbohydrate reserves. This study would provide another perspective into the effects of a reduced carbon supply on whole-tree physiological dynamics and how trees survive for decades with a reduced carbon supply. This research could also provide insight into how non-structural carbohydrate pools are affected under high demand for carbon and low water stress as a complement to current intensive research on the role of carbohydrate reserves in drought-related tree mortality.

Chapter 2

Tree-ring stable isotopes record the impact of a foliar fungal pathogen on CO₂ assimilation and growth in Douglas-fir

Abstract

Swiss needle cast (SNC) is a fungal disease of Douglas-fir (*Pseudotsuga menziesii* [Mirb.] Franco) with substantial economic ramifications that has recently become prevalent in coastal areas of the Pacific Northwest. Growth measurements and stable isotopes of carbon and oxygen in tree-rings of Douglas-fir and a non-susceptible reference species (western hemlock, *Tsuga heterophylla* (Raf.) Sarg.) were evaluated as potential proxies for variation in past SNC infection, particularly in relation to potential explanatory climate factors. Trees were sampled from a site where a fungicide trial took place from 1996 to 2000, which enabled the comparison of various parameters during years when disease was present and absent, relative to untreated trees which had the infection throughout the treatment period. Carbon stable isotope discrimination ($\Delta^{13}\text{C}$) of treated Douglas-fir tree-rings increased during the fungicide treatment period, and was ~ 1.6 ‰ greater than that of untreated Douglas-fir tree-rings during the final year of the fungicide treatment. Both annual growth and tree-ring $\Delta^{13}\text{C}$ increased with treatment such that treated Douglas-fir had values similar to co-occurring western hemlock during the treatment period, which suggests that the analysis of $\Delta^{13}\text{C}$ in Douglas-fir tree-rings may be a practical approach to tracking SNC disease history, provided a reference species is available to develop a parallel $\Delta^{13}\text{C}$

chronology. There was no difference in the tree-ring oxygen stable isotope ratio between treated and untreated Douglas-fir. Tree-ring $\Delta^{13}\text{C}$ of diseased Douglas-fir was negatively correlated with relative humidity (RH) during the two previous summers, consistent with increased leaf colonization by SNC under high humidity conditions that then leads to greater disease severity in following years.

Introduction

Swiss needle cast (SNC) disease of Douglas-fir (*Pseudotsuga menziesii* [Mirb.] Franco) is caused by stomatal blockages by the fruiting bodies (pseudothecia) of the fungus *Phaeocryptopus gaeumannii* (T. Rohde) Petr., which results in premature needle abscission (Manter *et al.*, 2000). SNC was present in the Pacific Northwest before it was considered an economically important disease. The first record of the fungus and SNC appears in the mid-1920s after a severe SNC epidemic of U.S.-imported Douglas-fir in Switzerland (Boyce, 1940). It was not until the late 1980s that the fungus began causing serious needle loss and growth reductions to Douglas-fir in the United States. Attempts to understand the potential influence of climate on the recent rise in disease severity have suggested that warm winter and spring temperatures and spring/summer leaf wetness may facilitate fungal growth and reproduction (Rosso & Hansen, 2003; Manter *et al.*, 2005; Coop & Stone, 2007; Latta *et al.*, 2009; Black *et al.*, 2010; Zhao *et al.*, 2011)

Previous research using Douglas-fir tree-ring widths attempted to identify historic SNC epidemics and the cause of the sudden prevalence of the disease in Oregon (Black *et al.*, 2010). Although Black *et al.* (2010) provide one potential avenue for understanding the history and onset of SNC in Oregon, tree-ring widths can be sensitive to numerous environmental variables that could confound a SNC signal or yield false positives for infection when there was no disease (*e.g.* climate signals, or disturbances associated with defoliating insect outbreaks, fires, windstorms, etc.; McCarroll & Loader, 2004; Barnard *et al.*, 2012). To more accurately quantify past SNC symptoms in tree-rings, a method is needed that can distinguish physiological responses to SNC from environmental noise. With this information, it would not only be possible to improve knowledge of the history of SNC in Oregon, but also to define clearer relationships between SNC symptoms and the climate factors that exacerbate them. As explained below, tree-ring stable isotope signatures should provide such information.

SNC restricts gas-exchange of Douglas-fir needles. In spring, spores land and germinate on current year foliage, and hyphae begin colonizing the needle surface and interior (Hansen *et al.*, 2000). Typically in the worst cases of infection, the fungus produces pseudothecia in the following spring that occlude stomata and reduce stomatal conductance (g_s) by about 83% and carbon assimilation rate (A) by about 72% by June (Manter *et al.*, 2000). The ratio of $[CO_2]$ within the chloroplasts (c_c) to that in the surrounding atmosphere (c_a) is modified by g_s and A , such that a decrease in g_s will cause c_c to decrease, and a decrease in A will cause c_c to increase (Farquhar *et*

al., 1989). $\Delta^{13}\text{C}$ is directly related to $c_c:c_a$, and thus, $\Delta^{13}\text{C}$ is also influenced by g_s and A (Farquhar, 1983; Evans *et al.*, 1986). The physical blockage of stomata in trees with SNC will cause a decline in A , but a stronger relative reduction in g_s , such that $c_c:c_a$ should decrease, causing the $\Delta^{13}\text{C}$ of fixed carbohydrates to decrease. In addition, the effect of reduced g_s in trees with SNC could likely cause changes in $\Delta^{18}\text{O}$ (Barbour, 2007). According to the original model of Farquhar and Lloyd (1993), a reduction in g_s would cause transpiration (E) to decrease, thus resulting in a decrease in the resistance of the path that water travels from the xylem to the site of evaporation near the stomatal pore. Therefore, there would be an increase in ^{18}O -enriched water at the site of carboxylation with decreased g_s , causing a potential increase in $\Delta^{18}\text{O}$ fixed into carbohydrates. Alternatively, sufficiently low levels of E , comparable to those reported for Douglas-fir (*e.g.* Cermak *et al.*, 2007), have been found to actually cause $\Delta^{18}\text{O}$ of leaf water to decrease with decreasing g_s (Song *et al.*, 2013). Taken together, because changes in g_s and A likely affect the $\Delta^{13}\text{C}$ and $\Delta^{18}\text{O}$ of carbohydrates fixed by diseased trees, tree-rings could record the signal imparted by the effects of SNC on g_s and A in a given year. If SNC indeed has an effect on tree-ring $\Delta^{13}\text{C}$ and/or $\Delta^{18}\text{O}$, then it is necessary to understand how $\Delta^{13}\text{C}$ and $\Delta^{18}\text{O}$ change in response to disease severity to be able to reconstruct past disease severity using these stable isotopes in tree-rings, and to better understand the response of the disease to meteorological variables.

The objectives of the present study were to determine: (1) whether analysis of tree-ring $\Delta^{13}\text{C}$ and/or $\Delta^{18}\text{O}$ can serve as a diagnostic tool for the detection of past SNC infection in Douglas-fir, and (2) which climate factors may modify the strength of the signal. Trees were sampled from the site of a fungicide trial where there are known years of severe SNC and years of low SNC. I hypothesized that $\Delta^{13}\text{C}$ would be higher in tree-rings during years of low SNC than during years of severe SNC. Likewise, I hypothesized that tree-ring $\Delta^{18}\text{O}$ during years of low SNC would be higher than that of years of severe SNC, based on the results of Song *et al.* (2013). For both carbon and oxygen analyses, co-occurring western hemlock (*Tsuga heterophylla* (Raf.) Sarg.) was used as a non-host reference species. Previous research suggests that severity of SNC infection increases under warmer winters and wetter springs and summers (*e.g.* greater fog, precipitation, RH), thus I expected to find lower $\Delta^{13}\text{C}$ and $\Delta^{18}\text{O}$ following winters with above average temperatures or wet conditions during spring and summer of the previous year.

Materials and methods

Carbon stable isotope conceptual approach

$\Delta^{13}\text{C}$ of plant cellulose ($\Delta^{13}\text{C}_{\text{cell}}$) as influenced by SNC was investigated because this signal should integrate, at the canopy-level, the physical and biochemical processes known to be affected by SNC at the leaf-level. Because the carbon isotope ratio of the atmosphere ($\delta^{13}\text{C}_{\text{atm}}$) changes over time and influences the carbon isotope ratio of

plant cellulose ($\delta^{13}\text{C}_{\text{cell}}$), this effect can then be accounted for by calculating $\Delta^{13}\text{C}_{\text{cell}}$ (‰), following Farquhar (1983):

$$\Delta^{13}\text{C}_{\text{cell}} = \frac{\delta^{13}\text{C}_{\text{atm}} - \delta^{13}\text{C}_{\text{cell}}}{1 + \delta^{13}\text{C}_{\text{cell}}}, \quad (\text{Eqn. 1})$$

where annual values of past $\delta^{13}\text{C}_{\text{atm}}$ have been estimated by McCarroll and Loader (2004; data from 1989 to 2003) and for more recent years from monitoring at Mauna Loa, Hawaii (<http://cdiac.ornl.gov/>; data from 2004 to 2011). C_3 photosynthesis causes $\Delta^{13}\text{C}_{\text{cell}}$ to be related directly to $c_c:c_a$, as described by Farquhar *et al.* (1989):

$$\Delta^{13}\text{C}_{\text{cell}} = a + (b - a) \left(\frac{c_c}{c_a} \right), \quad (\text{Eqn. 2})$$

where a is fractionation resulting from diffusion of CO_2 through the stomata and mesophyll (4.4‰), b is fractionation associated with carboxylation by rubisco (~27‰). Accordingly, $\Delta^{13}\text{C}_{\text{cell}}$ is influenced by increases in g_s and mesophyll conductance (g_m), which increase c_c ; as well as by A , which decreases c_c (Farquhar, 1983; Evans *et al.*, 1986; Farquhar *et al.*, 1989).

SNC infection starts in newly expanded leaves, but in areas with severe disease, it does not affect gas exchange until the pseudothecia emerge during early spring in the year following infection (Manter *et al.*, 2000; Stone *et al.*, 2008a). Photosynthetic assimilation rates in Douglas-fir are reduced via both stomatal limitations (physical blockage) and non-stomatal, biochemical limitations (Manter *et al.*, 2000). The physical blockage of stomata will cause a decline in A , but a stronger

relative reduction in g_s , such that $c_c:c_a$ should decrease, causing the $\Delta^{13}\text{C}$ of fixed carbohydrates to decrease.

There are potential limitations to the above scenario and therefore to the utility of tree-ring $\Delta^{13}\text{C}_{\text{cell}}$ values as integrators of temporal variation in the severity of SNC infection. SNC-induced biochemical limitations on assimilation rates may eventually cause $c_c:c_a$ to increase resulting in more positive $\Delta^{13}\text{C}_{\text{cell}}$ values. Additionally, hyphae in the leaf may continue to increase in mass through the summer following initial infection, causing further decreases in photosynthesis (Manter, 2000), which could cause the needles that experience the most severe symptoms to contribute less to tree-ring $\Delta^{13}\text{C}_{\text{cell}}$. Another consideration is that in the most extreme cases of infection, nearly all needles on the tree will develop a negative carbon balance (*i.e.* consuming more carbon than they fix) and will abscise during the second year of infection (Manter *et al.*, 2003a), thus reducing the impact of these needles on $\Delta^{13}\text{C}_{\text{cell}}$. Despite these potential caveats, the effect of the fungus on $\Delta^{13}\text{C}_{\text{cell}}$ should be strong enough to be detected in the wood due to the overwhelming presence and abundance of pseudothecia on diseased trees. As a precaution, the central portion of the tree-ring earlywood and latewood was used for analysis, hereafter referred to as *middlewood*, which contains cellulose synthesized from sugars produced in spring and early summer before abscission of the most severely infected needles.

A final consideration is the effect of the relationship between leaf mesophyll conductance (g_m) and $\Delta^{13}\text{C}_{\text{cell}}$. Flexas *et al.* (2008) restrict the definition of g_m to the diffusion of CO_2 through leaf mesophyll, including intercellular air spaces, the cell

wall, and the intracellular liquid pathway. Several studies have addressed how changes in g_m due to a variety of influences, such as water and nutrient stress, can lower c_c without a concurrent change in g_s (Flexas *et al.*, 2008; Seibt *et al.*, 2008; Flexas *et al.*, 2012). A reduction in c_c results in less discrimination against ^{13}C and a lower $\Delta^{13}\text{C}$, assuming there are no concurrent changes in the biochemical capacity of photosynthesis to offset the changes due to a reduction in g_m . Capitano (1999) demonstrated that there is significant hyphal growth inside the needles of Douglas-fir with SNC, which could potentially cause g_m to decrease, and thus $\Delta^{13}\text{C}_{\text{cell}}$ to decrease. The potential impact of the fungus on g_m should enhance the $\Delta^{13}\text{C}_{\text{cell}}$ signal in tree-rings by reducing c_c , although previous research with Douglas-fir has suggested that $\Delta^{13}\text{C}_{\text{cell}}$ should remain rather constant under changing g_m (Warren *et al.*, 2003). In either case, changes in g_m should not negatively affect the ability to use the analysis of $\Delta^{13}\text{C}_{\text{cell}}$ as a diagnostic tool for the detection of past SNC infection in Douglas-fir tree-rings, but it does limit the extent to which changes in $\Delta^{13}\text{C}_{\text{cell}}$ could be directly attributed to changes in g_s .

Oxygen stable isotope conceptual approach

We used stable isotope values of ^{18}O from the tree-ring cellulose of Douglas-fir as another potential indicator of variation in SNC infection. The carbohydrates that become tree-ring cellulose carry a signal imparted by the oxygen stable isotope ratio ($\delta^{18}\text{O}$) of leaf water, which is primarily influenced by the isotopic composition of source water entering the leaf from the xylem and ^{18}O -enrichment at the sites of

evaporation within the leaf (Craig & Gordon 1965; Dongmann *et al.* 1974). According to the Craig-Gordon model (Craig & Gordon 1965), the steady-state isotopic enrichment of oxygen over plant source water at the sites of evaporation in the leaf ($\Delta^{18}\text{O}_{\text{es}}$) is:

$$\Delta^{18}\text{O}_{\text{es}} = \varepsilon^+ + \varepsilon_k + (\Delta^{18}\text{O}_v - \varepsilon_k) \left(\frac{e_a}{e_l} \right), \quad (\text{Eqn. 3})$$

where ε^+ is the equilibrium fractionation factor between liquid water and gaseous water (*i.e.* vapor); ε_k is the kinetic fractionation factor as vapor diffuses from leaf intercellular spaces to the atmosphere; $\Delta^{18}\text{O}_v$ is the isotopic depletion of vapor relative to the plant source water; and $e_a:e_l$ is the ratio of atmospheric to intercellular vapor pressure.

Evaporative enrichment is complicated by several factors, such as the mass flow of unenriched water from the xylem that opposes the diffusion of enriched water from the sites of evaporation back toward the xylem (*i.e.* the Péclet effect; Farquhar & Lloyd 1993), which results in spatial heterogeneity in the isotopic composition of leaf water from the xylem to the site of evaporation (Wang & Yakir 1995). Evaporative enrichment is also affected by non-steady-state conditions (Farquhar & Cernusak 2005). Based on previous research that has shown little difference between steady- and non-steady-state models of leaf water enrichment in conifers (Lai *et al.* 2006; Seibt *et al.* 2006; Barnard *et al.* 2007; Snyder *et al.* 2010), we used the steady-state model for isotopic enrichment of mean lamina mesophyll water ($\Delta^{18}\text{O}_L$) proposed by Farquhar

and Lloyd (1993) for this study. $\Delta^{18}\text{O}_L$ is estimated using the equation (Farquhar & Lloyd, 1993):

$$\Delta^{18}\text{O}_L = \frac{\Delta^{18}\text{O}_e(1 - e^{-\wp})}{\wp}, \quad (\text{Eqn. 4})$$

where \wp is the Péclet number, a dimensionless ratio of the advection of unenriched source water to the back diffusion of enriched water from evaporative sites, which is calculated as follows:

$$\wp = \frac{EL}{CD}, \quad (\text{Eqn. 5})$$

where E is the leaf transpiration rate ($\text{mol m}^{-2} \text{s}^{-1}$), L is the effective path length (m) for water movement from the veins to the site of evaporation, C is the density of water (mol m^{-3}), and D is the diffusivity ($\text{m}^2 \text{s}^{-1}$) of H_2^{18}O in water. The parameter L is a product of the distance of the pathway from the xylem to the evaporative surface and a scaling factor that adjusts for the tortuosity of the path (Farquhar & Lloyd, 1993). Song *et al.* (2013) demonstrated in a study including a range of angiosperm and gymnosperm species that L is primarily driven by leaf physiology across species and is highly correlated to the inverse of transpiration ($1/E$). The authors hypothesize that when E is low (less than about $1 \text{ mmol m}^{-2} \text{s}^{-1}$), L increases exponentially because of a shift in the movement of water from an apoplastic (small L) to a symplastic pathway (large L).

The integration of $\Delta^{18}\text{O}_L$ into plant cellulose ($\Delta^{18}\text{O}_{\text{cell}}$) is described by the following equation (Barbour & Farquhar, 2000):

$$\Delta^{18}\text{O}_{\text{cell}} = \Delta^{18}\text{O}_L (1 - p_{\text{ex}} p_x) + \varepsilon_o, \quad (\text{Eqn. 6})$$

where p_{ex} is the proportion of oxygen atoms that exchange with xylem water during cellulose construction at the meristem, p_x is the proportion of unenriched xylem water at the site of cellulose construction (value of 1 when the cellulose was collected from mature, suberized stems), and ε_o is a fractionation factor of +27‰ to adjust for water/carbonyl exchange (Sternberg, 1989; Yakir & Deniro, 1990).

In the case of SNC, the effect of reduced g_s in Douglas-fir could likely cause changes in $\Delta^{18}\text{O}_{\text{cell}}$ in diseased trees. For this study, enrichment of plant cellulose with ^{18}O was referred to as $\delta^{18}\text{O}_{\text{cell}}$, without calculating the difference from source water ($\Delta^{18}\text{O}_{\text{cell}} = \delta^{18}\text{O}_{\text{cell}} - \delta^{18}\text{O}_{\text{sw}}$), because all sampled trees were located on the same site with the same primary source water and thus presumably have a constant offset from $\delta^{18}\text{O}_{\text{sw}}$ values. A reduction in g_s would also cause E to decrease, and according to the model of Farquhar and Lloyd (1993), should result in an increase in the $\delta^{18}\text{O}_{\text{cell}}$ due to the reduction of the Péclet effect. Alternatively, the data presented by Song *et al.* (2013) suggest that under a sufficient reduction in E , $\delta^{18}\text{O}_{\text{cell}}$ could decrease due to an exponential increase in L , especially since E is already relatively low in Douglas-fir (e.g. Cermak *et al.*, 2007). Furthermore, if the presence of *P. gaeumannii* in the leaf decreases g_m there could be an additional increase in L with SNC.

Field site and sampling

Trees were sampled in two Douglas-fir stands and one western hemlock stand at a coastal site near Beaver, Oregon (45.3°N, 123.8°W) where Douglas-fir trees exhibit chronic, severe SNC symptoms (Stone *et al.*, 2007). From 1996 to 2000, the Oregon Department of Forestry applied Bravo[®] fungicide (chlorothalonil) twice annually to the trees in one stand (treated Douglas-fir), which dramatically reduced SNC disease severity, while the trees in the other stand remained unsprayed (untreated Douglas-fir; Johnson *et al.*, 2003; Stone *et al.*, 2007). This experimental site thus provided a unique opportunity to quantify the impact of variation in SNC disease severity on tree-ring $\Delta^{13}\text{C}_{\text{cell}}$ and $\delta^{18}\text{O}_{\text{cell}}$ through comparative analyses of stable isotope chronologies in treated and untreated Douglas-fir prior to, during, and after fungicide application. The site severity index (site average of approximately 1.5 to 2 years of needle retention) was determined using the standard SNC sampling method (*e.g.* Maguire *et al.*, 2002; D.C. Shaw, pers. comm.). In January 2012, four increment cores (12 mm diameter) were collected from each of six trees of similar age, diameter at breast height (DBH), height, and crown width in both the fungicide treated stand and the untreated stand (Table 1). Four cores were collected from each of six trees in a nearby western hemlock stand to use as a baseline of climate impacts on stable isotope chronologies in a co-occurring species that does not become infected by SNC.

Additionally, twigs and foliage were collected from the terminal branches of six Douglas-fir trees at another coastal site with severe SNC near Tillamook, Oregon, called Prairie Hill (45.5°N, 123.8°W) to characterize the $\Delta^{13}\text{C}$ signal closer to the

source of carbohydrate synthesis in the crown. The branches were separated into segments representing growth increments from the years 2012, 2011, 2010, and 2009 (cohort years), and then separated into twigs and foliage. Bark and phloem were removed from the twigs to isolate the twig wood for isotopic analysis.

Annual growth analysis

Tree-core ring-widths were measured with a Velmex rotating measuring table and Measure J2X[®] measuring software. The cross-dating program COFECHA (Holmes, 1983; Grissino-Mayer, 2001) was used to identify missing and false rings. The ring widths for the four cores from each tree were averaged and basal area increment (BAI, cm²) was calculated to characterize annual tree growth from 1989 to 2011.

Stable isotope analyses

The middlewood was sliced from each tree-ring from 1989 to 2011 with a scalpel and ground into a fine powder using a ball-mill. Middlewood was defined as the portion of the ring that included the latter 75% of earlywood and the initial 25% of attached latewood from the same year. The ring material from all four cores from each tree was pooled to minimize the effect of differences in isotope signatures around the circumference of the tree. The α -cellulose of each tree-ring was isolated following Leavitt and Danzer (1993). The tree-ring $\delta^{13}\text{C}_{\text{cell}}$ and $\delta^{18}\text{O}_{\text{cell}}$ were measured by stable isotope ratio mass spectrometer (IRMS). $\delta^{13}\text{C}_{\text{cell}}$ measurements were carried out at Oregon State University (OSU) in the College of Earth, Ocean, and Atmospheric

Sciences (CEOAS) Stable Isotope Laboratory using a Carlo Erba NA1500 elemental analyzer connected to a DeltaPlus stable isotope mass spectrometer. $\delta^{18}\text{O}_{\text{cell}}$ measurements were carried out at the University of California, Davis, Stable Isotope Facility in the Department of Plant Sciences using an Elementar PyroCube (Elementar Analysensysteme GmbH) interfaced to a PDZ Europa 20-20 isotope ratio mass spectrometer (Sercon Ltd.). Measurement precision was better than 0.06‰ for $\delta^{13}\text{C}_{\text{cell}}$ and 0.24‰ for $\delta^{18}\text{O}_{\text{cell}}$ of tree-rings as determined from sample replicates.

Twig and foliage tissues were oven-dried and ground to a fine powder, packaged as whole tissue into tin capsules, and analyzed for $\delta^{13}\text{C}$ using an IRMS at the OSU CEOAS Stable Isotopes Laboratory. Measurement precision was better than 0.10‰ for $\delta^{13}\text{C}$ for twig and foliage tissues as determined from sample replicates. Current year needles are not expected to show significant fungus-induced alteration in their gas exchange, and thus, current year wood attached to current year foliage should not show an isotopic signal from the fungus. The $\Delta^{13}\text{C}$ signal in the newer wood on older growth increments that was built with carbohydrate produced by older needles was targeted for analysis because the effect of the fungus on needle physiology increases over time, and therefore, newer wood is expected to contain a stronger carbon isotope signal associated with fungal disruption of gas exchange. Since older tissues of twig wood are composed of different layers of wood made in different years, twig wood $\delta^{13}\text{C}$ values were adjusted with a calculation that estimated the $\delta^{13}\text{C}$ of wood produced in the most recent year for each growth increment cohort year. This calculation assumes that the amount of wood from each year was the same for growth

increments older than year 0, such that the calculated value of $\delta^{13}\text{C}$ for growth increment x ($\delta^{13}\text{C}_{\text{calc}x}$) based on the observed value for growth increment x ($\delta^{13}\text{C}_{\text{obs}x}$) where x equals the number of years beyond the sampling year (*i.e.* 0, 1, 2, 3 yr) was:

$$\delta^{13}\text{C}_{\text{calc}1} = (\delta^{13}\text{C}_{\text{obs}1} \times 2) - \delta^{13}\text{C}_{\text{obs}0}, \quad (\text{Eqn. 7})$$

$$\delta^{13}\text{C}_{\text{calc}2} = (\delta^{13}\text{C}_{\text{obs}2} \times 3) - \delta^{13}\text{C}_{\text{obs}0} - \delta^{13}\text{C}_{\text{calc}1}, \quad (\text{Eqn. 8})$$

$$\delta^{13}\text{C}_{\text{calc}3} = (\delta^{13}\text{C}_{\text{obs}3} \times 4) - \delta^{13}\text{C}_{\text{obs}0} - \delta^{13}\text{C}_{\text{calc}1} - \delta^{13}\text{C}_{\text{calc}2}. \quad (\text{Eqn. 9})$$

Values of $\delta^{13}\text{C}_{\text{calc}}$ were transformed to $\Delta^{13}\text{C}$ using the procedure described above for tree-ring $\delta^{13}\text{C}_{\text{cell}}$.

Climate data

Climate data, including monthly and annual average precipitation, temperature, and dew point, were obtained from the PRISM Climate Group at Oregon State University (<http://prism.oregonstate.edu>). Average monthly and annual RH values were calculated from temperature and dew point temperature values. Fog occurrence data were acquired from J. Johnstone, using the methods employed by Johnstone and Dawson (2010). The average fog frequencies of the Southwest Oregon Regional Airport in North Bend, Oregon, and of the Astoria Regional Airport in Warrenton, Oregon, were calculated and averaged to determine the monthly and annual average

fog frequency for the Oregon coast. Growing season averages included data from May through July, and summer averages included data from June through September.

Statistical analyses

Three separate repeated measures ANOVA tests with an AR1 covariance structure were used to determine the difference in mean BAI, as well as mean tree-ring $\Delta^{13}\text{C}_{\text{cell}}$ and $\delta^{18}\text{O}_{\text{cell}}$, between treated and untreated Douglas-fir, and western hemlock, at the Beaver site for each year from 1989 to 2011. A linear model using generalized least squares with an AR1 covariance structure was used to compare the relationship between mean tree-ring $\Delta^{13}\text{C}$ and mean BAI for the treated Douglas-fir trees. Another linear model using generalized least squares with an AR1 covariance structure was used to describe and compare mean $\Delta^{13}\text{C}$ of twig wood, and foliage, from the Prairie Hill site with increasing tissue age.

To detect the impact of climate on disease severity, climate influences (mean monthly temperature, precipitation, RH, and fog occurrence) were analyzed on the two tree-ring stable isotope series of each species (mean tree-ring $\Delta^{13}\text{C}_{\text{cell}}$ and $\delta^{18}\text{O}_{\text{cell}}$ of untreated Douglas-fir and western hemlock) using Pearson's correlation coefficients (r). Correlations with a magnitude of at least 0.42 corresponds approximately with the 95% confidence level for a Gaussian white noise process ($n = 23$ years; 1989-2011), so any correlation exceeding ± 0.42 was considered significant and an indicator of an important relationship to inform interpretation of the data.

Results

Annual growth

Due to the significant interaction between the effect of treatment and year on mean annual BAI ($F_{22, 230} = 4.79$, $P = 0.0001$), the rest of the analyses discussed below will describe a difference in mean annual BAI between treatments for each year of observation separately. The annual growth trajectories of the treated and untreated Douglas-fir were essentially indistinguishable before imposing the fungicide treatment in 1996 (Fig. 2.1). There was a one-year lag before BAI differed between treatments after treatment began. Mean annual BAI of the fungicide-treated Douglas-fir was significantly greater than that of untreated Douglas-fir beginning in the second year of treatment (1997) and increased each year until a peak average difference of about 27.4 cm² (95% CI: [19.4, 35.5]) in the final year of treatment (2000). Thereafter, growth of the treated trees declined over three years until 2004 when there was no longer a statistically significant difference between treated and untreated trees.

Branch carbon stable isotopes

At the Prairie Hill site where branches were collected from Douglas-fir trees with severe SNC, there was a significant interaction between tissue type (twig wood or foliage) and growth increment age on mean $\Delta^{13}\text{C}$ ($F_{1, 41} = 12.84$, $P = 0.001$), so the rate of change in $\Delta^{13}\text{C}$ per increase in growth increment age for twig wood and foliage will be discussed separately in this analysis. The mean $\Delta^{13}\text{C}$ of twig wood decreased with tissue age by about 1.08‰ per cohort year (95% CI: [-1.27, -0.89]), and the mean

$\Delta^{13}\text{C}$ of foliage decreased by about 0.56‰ per cohort year (95% CI: [-0.77, -0.34]) (Fig. 2.2).

Tree-ring carbon stable isotopes

There was a significant interaction between treatment (treated Douglas-fir, untreated Douglas-fir, western hemlock) and year of observation on mean tree-ring $\Delta^{13}\text{C}_{\text{cell}}$ (1989-2011; $F_{44, 325} = 1.54$, $P = 0.02$), so differences in mean tree-ring $\Delta^{13}\text{C}_{\text{cell}}$ between treatment groups will be discussed separately for each year. The mean tree-ring $\Delta^{13}\text{C}_{\text{cell}}$ of treated Douglas-fir became steadily greater after treatment began in 1996, and was significantly greater than untreated Douglas-fir from 1999 to 2002 (Fig. 2.3). The mean difference in tree-ring $\Delta^{13}\text{C}_{\text{cell}}$ between treated and untreated Douglas-fir reached a maximum in 2001 (about 1.59‰; 95% CI: [0.66, 2.52]), and thereafter declined until there was no statistically significant difference between treated and untreated Douglas-fir in 2003.

Mean tree-ring $\Delta^{13}\text{C}_{\text{cell}}$ differed significantly between treated Douglas-fir and western hemlock from 1989 to 1995 by about 1.81‰, but from the year that treatment began through three years following the end of treatment (1996 to 2003), there was no statistically significant difference between these two groups (Figure 2.3). Following 2003 and to the end of the observation period in 2011, there was a significant difference in mean tree-ring $\Delta^{13}\text{C}_{\text{cell}}$ between treated Douglas-fir and western hemlock. Mean tree-ring $\Delta^{13}\text{C}_{\text{cell}}$ values between untreated Douglas-fir and western hemlock were significantly different in every year of the observation period except for two

years (1989 and 2000). The mean difference in $\Delta^{13}\text{C}_{\text{cell}}$ between untreated Douglas-fir and western hemlock was about 1.39‰.

The relationship between mean BAI and mean tree-ring $\Delta^{13}\text{C}$ of treated Douglas-fir over the observation period (1989 to 2011) was such that BAI increased by 9.57 cm² for every 1‰ increase in $\Delta^{13}\text{C}_{\text{cell}}$ (95% CI: [5.36, 13.78], $P=0.0002$; Fig. 2.4).

Tree-ring oxygen stable isotopes

There was not a significant interaction between treatment (treated Douglas-fir, untreated Douglas-fir, western hemlock) and year of observation on mean tree-ring $\delta^{18}\text{O}_{\text{cell}}$ between 1989 and 2011 ($F_{22, 367}=1.40$, $P=0.06$; Fig. 2.5). After accounting for year of treatment, there was no significant difference in mean tree-ring $\delta^{18}\text{O}_{\text{cell}}$ between treated and untreated Douglas-fir (Fig. 2.5). The mean tree-ring $\delta^{18}\text{O}_{\text{cell}}$ of western hemlock was about 0.61‰ greater than that of treated Douglas-fir (95% CI:[0.38, 0.84]), and about 0.60‰ greater than that of untreated Douglas-fir (95% CI:[0.37, 0.82]; Fig. 2.5).

Climate Analyses

Due to the lack of difference in mean tree-ring $\delta^{18}\text{O}_{\text{cell}}$ between treatments during the treatment period, and thus the absence of evidence in support of using tree-ring $\delta^{18}\text{O}_{\text{cell}}$ as an indicator of variability in SNC disease severity, only tree-ring $\Delta^{13}\text{C}_{\text{cell}}$ is discussed in the climate analyses. There was a significant negative correlation between

average previous December temperature and $\Delta^{13}\text{C}_{\text{cell}}$ of western hemlock ($r = -0.47$; Fig. 2.6). Previous July precipitation displayed a positive correlation with $\Delta^{13}\text{C}_{\text{cell}}$ of untreated Douglas-fir ($r = 0.43$). There were also significant positive relationships between previous December fog occurrence and $\Delta^{13}\text{C}_{\text{cell}}$ of untreated Douglas-fir ($r = 0.51$). The strongest significant correlations were between RH in the previous June, July, August, and September, growing season, summer, and two-years-previous summer, and $\Delta^{13}\text{C}_{\text{cell}}$ of untreated Douglas-fir ($r = -0.51, -0.49, -0.54, -0.57, -0.51, -0.62, -0.60$, respectively), indicating that $\Delta^{13}\text{C}_{\text{cell}}$ decreased with increasing humidity of the previous years. There were no significant correlations between RH and $\Delta^{13}\text{C}_{\text{cell}}$ of western hemlock.

Discussion

Annual BAI of treated Douglas-fir increased soon after the fungicide treatment began and was more than twice that of untreated trees by the fifth year of treatment (Fig. 2.1). Tree-ring $\Delta^{13}\text{C}_{\text{cell}}$ of treated Douglas-fir (low SNC) was greater than that of untreated Douglas-fir (severe SNC) from the fourth year of treatment through two years after treatment ended, reaching a peak difference of about 1.5‰ in 2001 (Fig. 2.3). The increase in $\Delta^{13}\text{C}_{\text{cell}}$ following the fungicide treatment and the near elimination of SNC was consistent with decreased diffusional limitation on needle gas exchange. Evidence of a cumulative effect of *P. gaeumannii* on $\Delta^{13}\text{C}$ of tissues was found in the canopy, where older twig wood and foliage had lower $\Delta^{13}\text{C}$ than newer tissues (Fig. 2.2). The relationship between BAI and tree-ring $\Delta^{13}\text{C}_{\text{cell}}$ (Fig. 2.4)

demonstrated that treated Douglas-fir had values similar to western hemlock during the treatment period, which suggests that the use of $\Delta^{13}\text{C}_{\text{cell}}$ in Douglas-fir tree-rings may be a practical technique for tracking SNC disease history, provided a suitable, co-occurring, non-infected reference species like western hemlock is also used to develop a reference $\Delta^{13}\text{C}_{\text{cell}}$ chronology. In contrast to the tree-ring $\Delta^{13}\text{C}_{\text{cell}}$ results, there were no distinguishable differences in tree-ring $\delta^{18}\text{O}_{\text{cell}}$ between treated and untreated Douglas-fir during the years of the fungicide treatment and both are offset by $\sim 0.6\text{‰}$ from western hemlock (Fig. 2.5). It appears that when tree-ring $\Delta^{13}\text{C}_{\text{cell}}$ was used as a proxy for disease severity in Douglas-fir, disease severity was most strongly correlated with high RH in previous summer and growing season months (Fig. 2.6).

Annual growth and carbon stable isotopes

In agreement with previous research at the Beaver site, annual growth of treated Douglas-fir increased in response to the fungicide treatment (Johnson *et al.*, 2003). A one-year lag was identified in the annual growth response after the first year of treatment, as well as a three-year lag in the return to pre-treatment growth levels after the last year of treatment. These lags are likely due to the nature of the life cycle of *P. gaeumannii* and the progression of disease in Douglas-fir foliage. After initial infection of current-year foliage, it takes at least a year for *P. gaeumannii* to produce the pseudothecia that result in disease symptoms that include reduced carbon dioxide assimilation and foliage loss. Thus, it would take a year after the first application of fungicide for there to be a notable difference in foliage retention and annual growth

between treated and untreated trees. Furthermore, because the fungus only infects new foliage, each subsequent year of treatment meant that the treated trees had one more cohort of healthy, productive foliage, which explains why annual growth steadily increased over the treatment period and why there was a one-year lag before annual growth began to decline back to pre-treatment levels after the last year of treatment. Needle retention on the coast is anywhere between three and four needle cohorts for healthy Douglas-fir (Shaw *et al.*, 2011), so the three-year lag before annual growth of treated trees returned to pre-treatment levels after the final year of treatment represents the steady annual progression of additional diseased needle cohorts in the absence of the fungicide treatment.

The response of tree-ring $\Delta^{13}\text{C}_{\text{cell}}$ to fungicide treatment over time was similar to the pattern in annual growth. There was a difference in the number of years that BAI and tree-ring $\Delta^{13}\text{C}_{\text{cell}}$ between treated and untreated trees were significantly different, such that there was a three-year lag after treatment began and a two-year lag after treatment ended for tree-ring $\Delta^{13}\text{C}_{\text{cell}}$. It is possible that additional healthy needle cohorts were required to produce a significant change in tree-ring $\Delta^{13}\text{C}_{\text{cell}}$ than was required to produce changes in annual growth, which could explain why the difference in $\Delta^{13}\text{C}_{\text{cell}}$ between Douglas-fir treatment groups required more time to manifest after treatment began and less time to diminish after treatment ended. Nevertheless, the overall trajectory of the tree-ring $\Delta^{13}\text{C}_{\text{cell}}$ response to treatment was essentially consistent with that of annual growth.

The $\Delta^{13}\text{C}_{\text{cell}}$ signal that was identified in tree-rings was also present in the crown at the source of carbohydrate synthesis. Foliage and twig wood $\Delta^{13}\text{C}$ values were clearly different, which has been shown in previous research to be related to tissue type (reviewed by Cernusak *et al.*, 2009). Non-photosynthetic tissues, such as those found in branch and stem wood, are typically enriched in $\Delta^{13}\text{C}$ by between 1‰ and 3‰ compared to leaves on the same branch or tree (Cernusak *et al.*, 2009). The difference in $\Delta^{13}\text{C}$ between foliage and twig wood fell within this range for most tissue ages, though older growth increments tended to have slightly greater differences in $\Delta^{13}\text{C}$ than 3‰. The $\Delta^{13}\text{C}$ of conifer foliage can decrease by 0.01-0.50‰ per year due to natural constraints on stomatal conductance that increase from the branch tip to base (Warren & Adams, 2000; Panek, 1996). Because the secondary growth of twigs is derived from carbohydrate exported from needles attached to them, the $\Delta^{13}\text{C}$ of both tissues should decrease over time at roughly the same rate. The results for foliar $\Delta^{13}\text{C}$ fell slightly outside the maximum of this range (0.56‰ per cohort year), and there was actually a difference in the rate of decline in $\Delta^{13}\text{C}$ with cohort year between foliage and twig wood, such that twig wood declined about twice the rate of foliage (1.1‰ per cohort year for twig wood). The bulk mass of foliage is cellulose that is laid down in the first year when SNC is still in the early stages of inoculation. Foliar cellulose does not turn over, so any change in foliar $\Delta^{13}\text{C}$ with increasing age must be associated with leaf constituents that are produced after the needle is developed (*e.g.* non-structural carbohydrate and other substances that undergo metabolic turnover) and produced under constrained stomatal conductance, be it natural or disease-related. The observed

larger than average decrease in foliar $\Delta^{13}\text{C}$ with age is likely due to the additional effects of disease, namely the larger fraction of occluded stomata and concurrent decrease in stomatal conductance with each year following initial infection as the fungus grows and produces more pseudothecia (Hansen *et al.*, 2000; Manter *et al.*, 2003a). Furthermore, the exported carbohydrate from foliage and the secondary growth of the attached twig that it ultimately builds would have progressively lower $\Delta^{13}\text{C}$ with each cohort year. Thus, diseased twig wood would be expected to have a greater rate of decrease in $\Delta^{13}\text{C}$ with age compared to foliage since the exported carbohydrate from older needles would have a lower $\Delta^{13}\text{C}$ signal than the bulk mass of the needle itself.

Mean tree-ring $\Delta^{13}\text{C}_{\text{cell}}$ of treated Douglas-fir and western hemlock were not significantly different from the year treatment began through three years following treatment, which roughly follows the trend in significant differences between the mean tree-ring $\Delta^{13}\text{C}_{\text{cell}}$ of treated and untreated Douglas-fir that were observed during and after the treatment period. When the positive relationship between mean tree-ring $\Delta^{13}\text{C}_{\text{cell}}$ and BAI of treated trees was examined, values of $\Delta^{13}\text{C}_{\text{cell}}$ and BAI during the treatment period were found to be more like the mean $\Delta^{13}\text{C}_{\text{cell}}$ and BAI values of western hemlock (Fig. 2.4). These results suggest that there is clear potential in using tree-ring $\Delta^{13}\text{C}_{\text{cell}}$ and BAI chronologies as a means to track SNC disease history on the Oregon coast provided a suitable co-occurring reference species like western hemlock is available. Applying this method, years where disease was low or absent within a Douglas-fir tree-ring $\Delta^{13}\text{C}_{\text{cell}}$ chronology would not be significantly different from the

same years in a tree-ring $\Delta^{13}\text{C}_{\text{cell}}$ chronology of nearby western hemlock, and the degree of divergence in tree-ring $\Delta^{13}\text{C}_{\text{cell}}$ of the two species in a given year should be related to SNC disease severity for that year. It would be beneficial to use BAI in conjunction with tree-ring $\Delta^{13}\text{C}_{\text{cell}}$ since both variables appear to track variation in disease severity and could potentially identify non-SNC influences when one variable changes while the other remains constant.

Oxygen stable isotopes

Contrary to my hypothesis, no difference in mean tree-ring $\delta^{18}\text{O}_{\text{cell}}$ was found between treated and untreated Douglas-fir in response to treatment. Previous research has demonstrated that high RH (~60-70%) can mask the effects of reduced stomatal conductance on $\delta^{18}\text{O}_L$, and thus the signal imparted to tree-ring cellulose, because there is so little evaporative enrichment of leaf water and the isotopic exchange with atmospheric vapor is much higher under high RH (Roden & Ehleringer, 1999; Barbour & Farquhar, 2000; Brooks & Mitchell, 2011). Equations 3-6 were used to explore the effects of variation in g_s and L (effective path length) on $\Delta^{18}\text{O}_{\text{cell}}$ under the mean growing season RH at the study site (78%, May-July). A reference value for g_s of $0.14 \text{ mol m}^{-2} \text{ s}^{-1}$, typical for healthy, non-water-limited Douglas-fir was applied (Bond & Kavanagh, 1999). Stomatal conductance was then varied between 0 and $0.14 \text{ mol m}^{-2} \text{ s}^{-1}$ with L set between 33 and 2400 mm, representative of the range of L reported for several conifer species (Wang *et al.*, 1998; Song *et al.*, 2013). Source water $\delta^{18}\text{O}$ was set to the five-year average for precipitation in Newport, Oregon (-7.05‰; J.R.

Brooks, pers. comm.). Leaf and air temperature were set for average summer time conditions determined from the PRISM climate data as 15°C. Boundary layer conductance was set to $2 \text{ mol m}^{-2} \text{ s}^{-1}$. $\Delta^{18}\text{O}_V$ was assumed to be in equilibrium with source water, and therefore was equal to $-\varepsilon^+$ (Barbour, 2007). Finally, in equation 6, p_{ex} was set to 0.4 and p_x to 1 (Brooks & Mitchell, 2011).

The results of this modeling exercise (Fig. 2.7) suggest that even under near complete loss of stomatal conductance in diseased trees, the difference in $\Delta^{18}\text{O}_{\text{cell}}$ between diseased and healthy trees with a typical L (33mm) would only be about 0.46‰. Moreover, Manter *et al.* (2000) found that Douglas-fir seedlings with SNC that were sampled in May and June had g_s values of around 0.02-0.05 $\text{mol m}^{-2} \text{ sec}^{-1}$, while control seedlings had values around 0.08-0.12 $\text{mol m}^{-2} \text{ s}^{-1}$. Although mature Douglas-fir was sampled, and not seedlings, it is possible that the magnitude of difference in g_s between treated and untreated trees was not as great as in this modeling exercise, thus yielding an even smaller difference in $\delta^{18}\text{O}_{\text{cell}}$ between treatments. Furthermore, the model demonstrates that as L increases there should be an increase in the difference in $\Delta^{18}\text{O}_{\text{cell}}$ from the control value. Although L may be slightly modified by the presence of the fungus in the needle, the lack of difference in the observed tree-ring $\delta^{18}\text{O}_{\text{cell}}$ between treated and untreated Douglas-fir suggests that any difference in L between treatments was minimal.

In summary, the blockage of stomata by pseudothecia and/or hyphae within the leaf mesophyll may indeed affect $\delta^{18}\text{O}_{\text{cell}}$ when RH is low, but because RH was rather high at the study site, any influence of the fungus on $\delta^{18}\text{O}_{\text{cell}}$ was not observed. Since

SNC is more prevalent in coastal Oregon where RH is normally high, the results of the present study imply that stable isotopes of oxygen in tree-rings would not serve as a reliable indicator of variability in SNC disease severity.

Disease severity and climate

The climate variables found to have the strongest relationships with disease severity (measured as Douglas-fir tree-ring $\Delta^{13}\text{C}_{\text{cell}}$) were previous summer and growing season averages of RH (previous June, July, August, September, growing season, and summer; and two summers previous). The strongest of these correlations were with RH of the previous summer ($r = -0.62$) and two summers previous ($r = -0.60$). A typical physiological response of healthy trees to low RH (and thus, high E) is to close stomata, causing $\Delta^{13}\text{C}_{\text{cell}}$ to decrease. In the case of Douglas-fir with SNC, the opposite was observed; low RH was related to increased $\Delta^{13}\text{C}_{\text{cell}}$. Previous research has shown that spring and summer leaf wetness in the year of initial infection is positively correlated with disease severity (Hansen *et al.*, 2000; Rosso & Hansen, 2003; Manter *et al.*, 2005; Latta *et al.*, 2009), which is likely due to increased spore germination on leaf surfaces. The negative relationship between previous summer RH and Douglas-fir tree-ring $\Delta^{13}\text{C}_{\text{cell}}$ likely reflects higher leaf wetness through increased nightly dew formation and lower evaporation when the spores are germinating. In turn greater leaf wetness, particularly from dew that would presumably wash off fewer spores than rainfall, would promote greater spore adhesion to needles and more successful germination on foliage. Subsequent increases in pseudothecia-blocked

stomata would result in lower $\Delta^{13}\text{C}_{\text{cell}}$ in the following year or two when that foliage would be contributing substantial photosynthate. Accordingly, this response would not be observed in a species that is not susceptible to SNC, like western hemlock, which did not demonstrate any relationship between RH and tree-ring $\Delta^{13}\text{C}_{\text{cell}}$.

As mentioned previously, variation in SNC disease severity has primarily been correlated with warm winter temperatures and wet spring and summer conditions, with some studies also reporting a negative relationship between high summer temperatures and disease severity (Rosso & Hansen, 2003; Zhao *et al.*, 2011). Although the results of the present study agreed with the positive relationship between July RH and disease severity reported by Latta *et al.* (2009), there was no evidence for a relationship between temperature, precipitation, or fog occurrence and disease severity as measured with tree-ring $\Delta^{13}\text{C}_{\text{cell}}$. The relationship between climate and SNC severity in past studies has been explored using different measures of disease, such as needle retention (Hansen & Rosso, 2003; Coop & Stone, 2007; Latta *et al.*, 2009; Zhao *et al.*, 2011), pseudothecia abundance (Manter *et al.*, 2005), and growth (*i.e.* tree-ring width; Black *et al.* 2010). Although these measures are reasonable assessments of disease signs and symptoms, some have potential confounding factors that could complicate efforts to determine their respective relationships to climate. For example, needle retention can be influenced by stand density, tree age, temperature, water availability, nutritional status, herbivory, and functional net photosynthesis (*reviewed by* Chabot & Hicks, 1982; Ewers & Schmid, 1981; Pouttu & Dobbertin, 2000; Xiao, 2003), and tree-ring widths are sensitive to a variety of environmental signals (McCarroll &

Loader, 2004) independent of disease severity. Although there are certainly factors other than SNC that could potentially affect tree-ring $\Delta^{13}\text{C}_{\text{cell}}$, differences in carbon stable isotope signatures of diseased Douglas-fir and a healthy reference species may eliminate noise contributed by other factors that affect needle retention and tree-ring width and provide another perspective of the relationship between climate and SNC disease severity.

The results of the present study demonstrated that SNC causes reduced $\Delta^{13}\text{C}_{\text{cell}}$ values. However, without information regarding disease status, these results could be interpreted very differently with traditional stable isotope theory, particularly when attempting climate reconstruction with tree-ring stable isotopes. Thus, future related studies should consider the potential impacts of disease when interpreting stable isotope signals in tree-rings.

Acknowledgments

This research was supported in part by NSF grant DEB-073882 and a grant from the Swiss Needle Cast Cooperative. Special thanks to Alan Kanaskie of ODF for site access; Danielle Marias, Joshua Petitmermet, Ben Roberts-Pierel, Holly Kearns, Kristen Falk, and Regina Kurapova for their invaluable work in the field and lab; J. Johnstone for access to coastal Oregon fog data; and Lisa Ganio, Ariel Muldoon, and Julia Burton for statistical consulting.

Table 2.1 Characteristics of each treatment group (n=6 for each group), including age (determined from cores), diameter at breast height (DBH), height, and crown width (diameter) with one standard deviation from the mean in parentheses.

Treatment Group	Age (years)	DBH (cm)	Height (m)	Crown width (m)
Treated Douglas-fir	29 (2)	31.7 (1.2)	22.2 (1.0)	6.7 (0.7)
Untreated Douglas-fir	28 (1)	28.0 (4.2)	19.7 (1.4)	5.0 (1.0)
Western hemlock	23 (4)	37.0 (9.3)	21.4 (2.5)	5.3 (1.5)

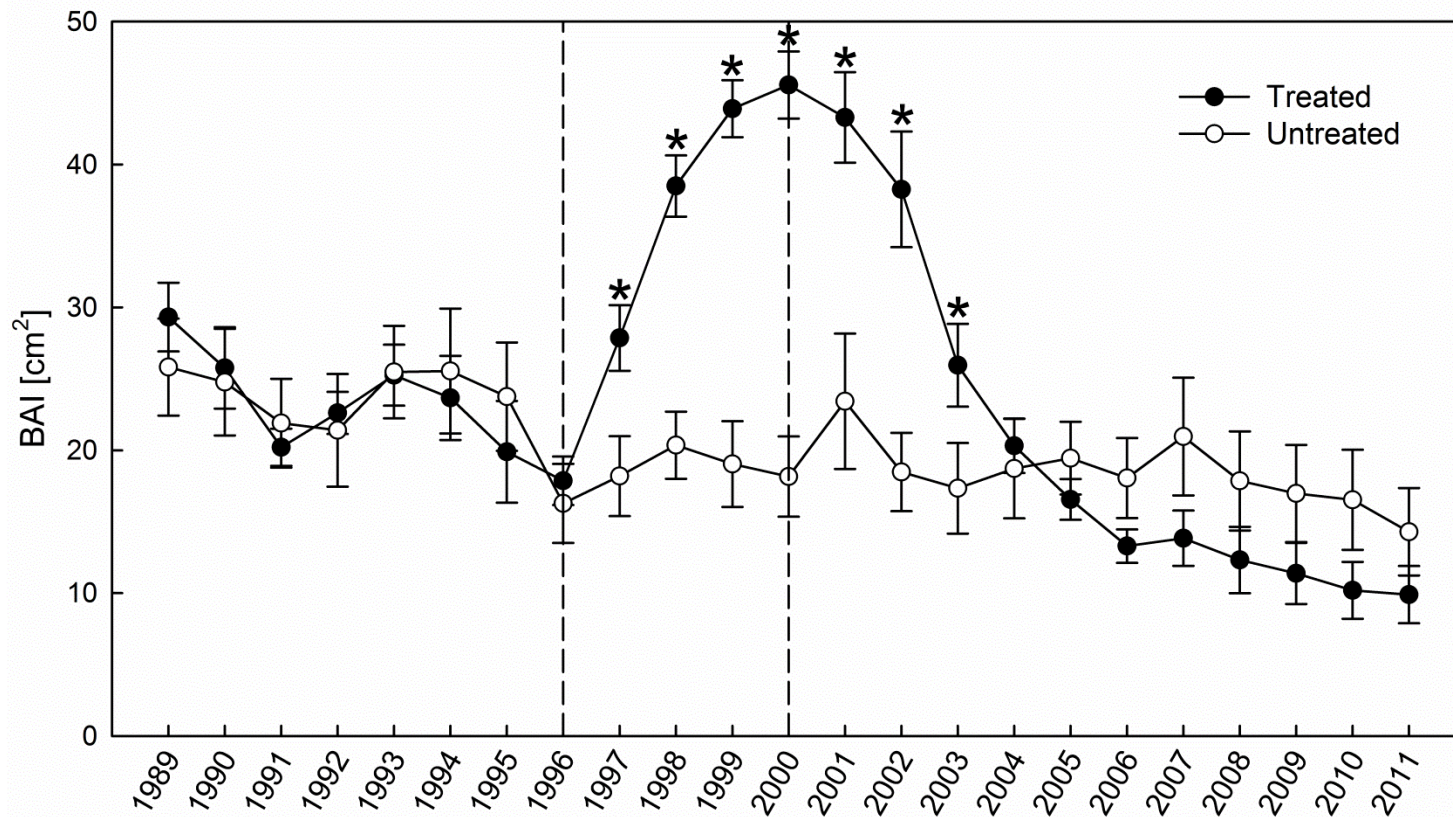


Figure 2.1 Mean basal area increment (BAI) of fungicide-treated and untreated Douglas-firs at the Beaver, Oregon site during the years of observation (1989-2011; $n=6$ trees per treatment). The treatment period is indicated by vertical dashed lines (1996-2000, inclusive). Bars represent one standard error. Asterisks indicate years of significant difference between treated and untreated Douglas-fir (results of repeated-measures ANOVA with an AR1 covariance structure).

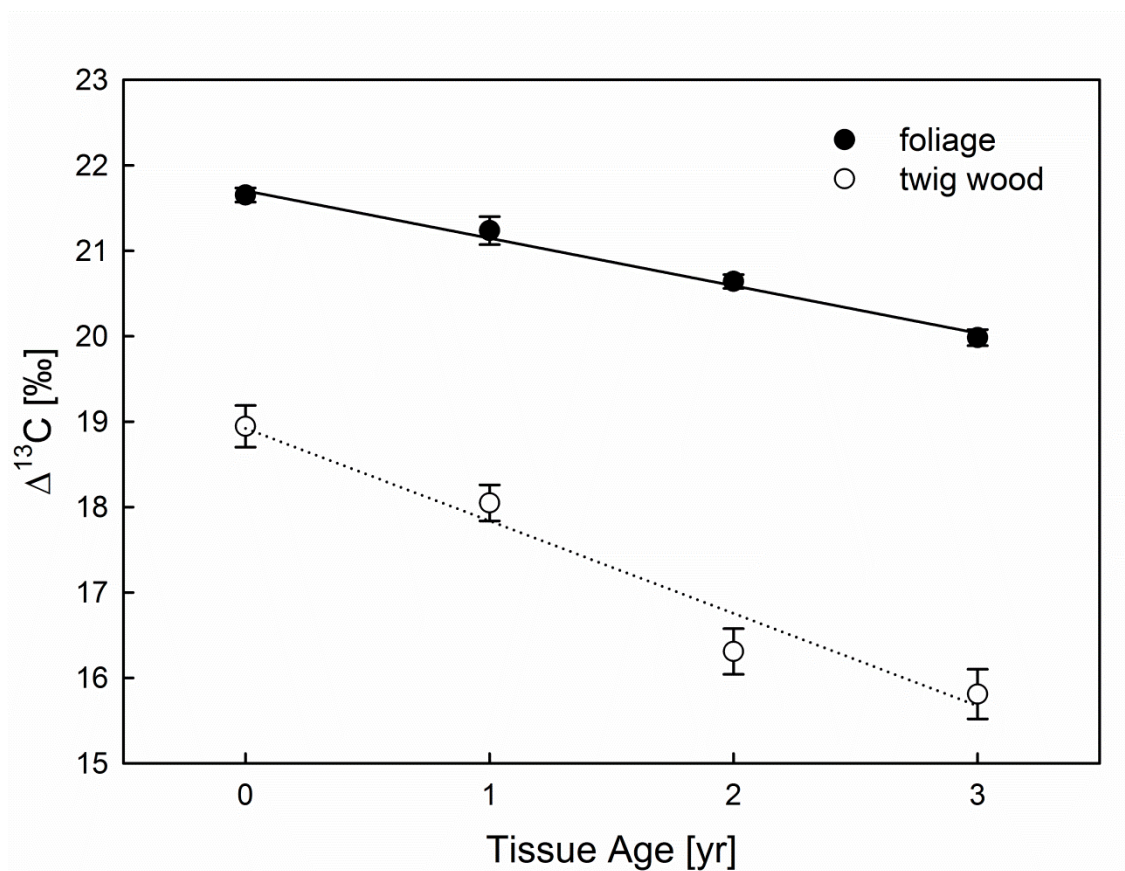


Figure 2.2 $\Delta^{13}\text{C}$ of foliage and twig wood samples from branch cohorts aged 0 to 3 years old at the Prairie Hill site ($n=6$ trees). Lines represent the regression results of a general least squares model with an AR1 covariance structure fit to foliage (solid) and twig wood (dotted; $P=0.001$). Twig wood values were adjusted as described in Materials and Methods. Bars represent one standard error.

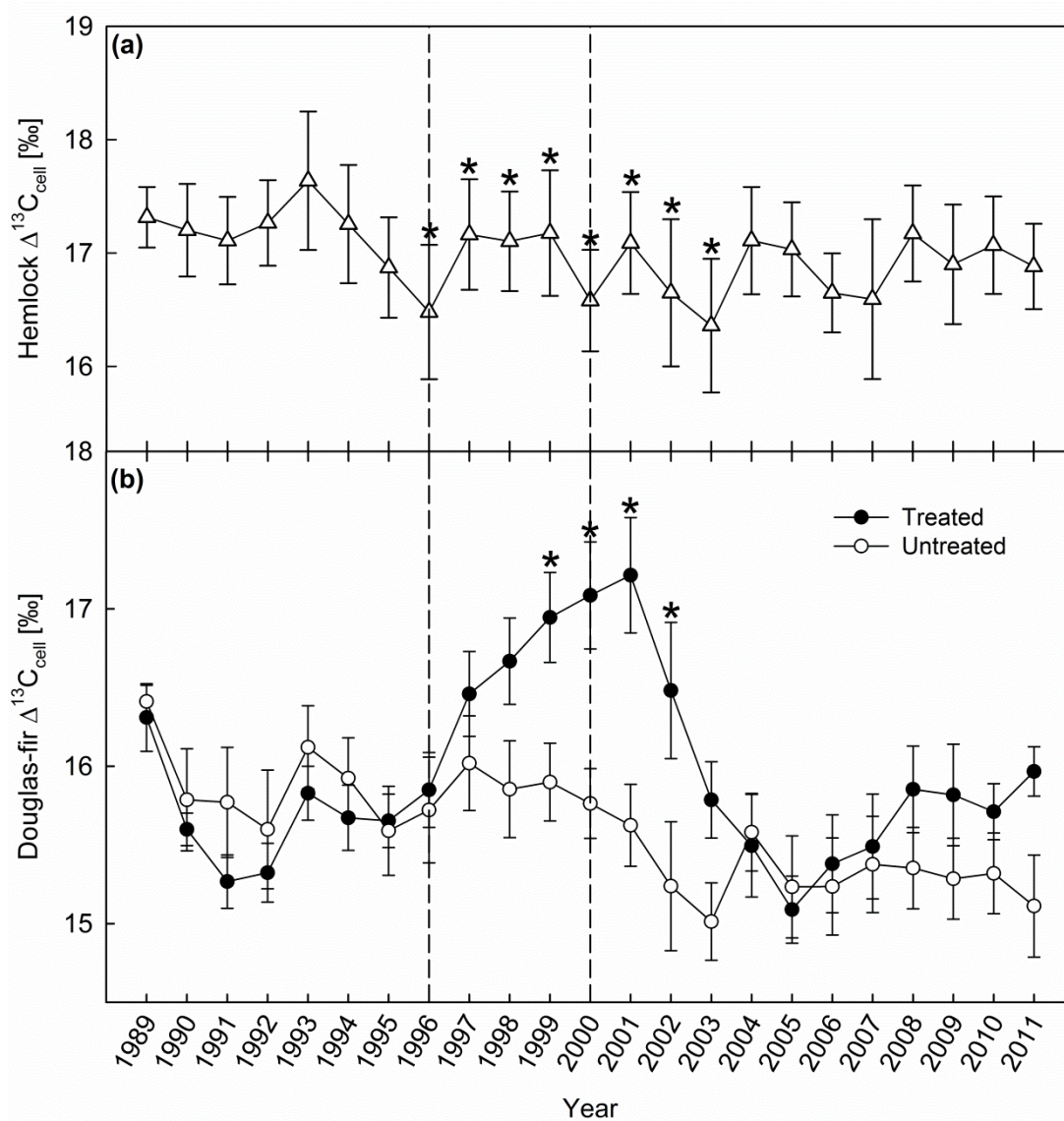


Figure 2.3 Mean $\Delta^{13}\text{C}_{\text{cell}}$ of western hemlock (a), and fungicide-treated and untreated Douglas-firs (b) at the Beaver, Oregon site during the years of observation (1989-2011; $n=6$ trees per treatment). The treatment period is indicated by vertical dashed lines (1996-2000, inclusive). Bars represent one standard error. Asterisks in (a) indicate years of no difference between western hemlock and treated Douglas-fir, and in (b) indicate years of significant difference between treated and untreated Douglas-fir (results of repeated-measures ANOVA with an AR1 covariance structure).

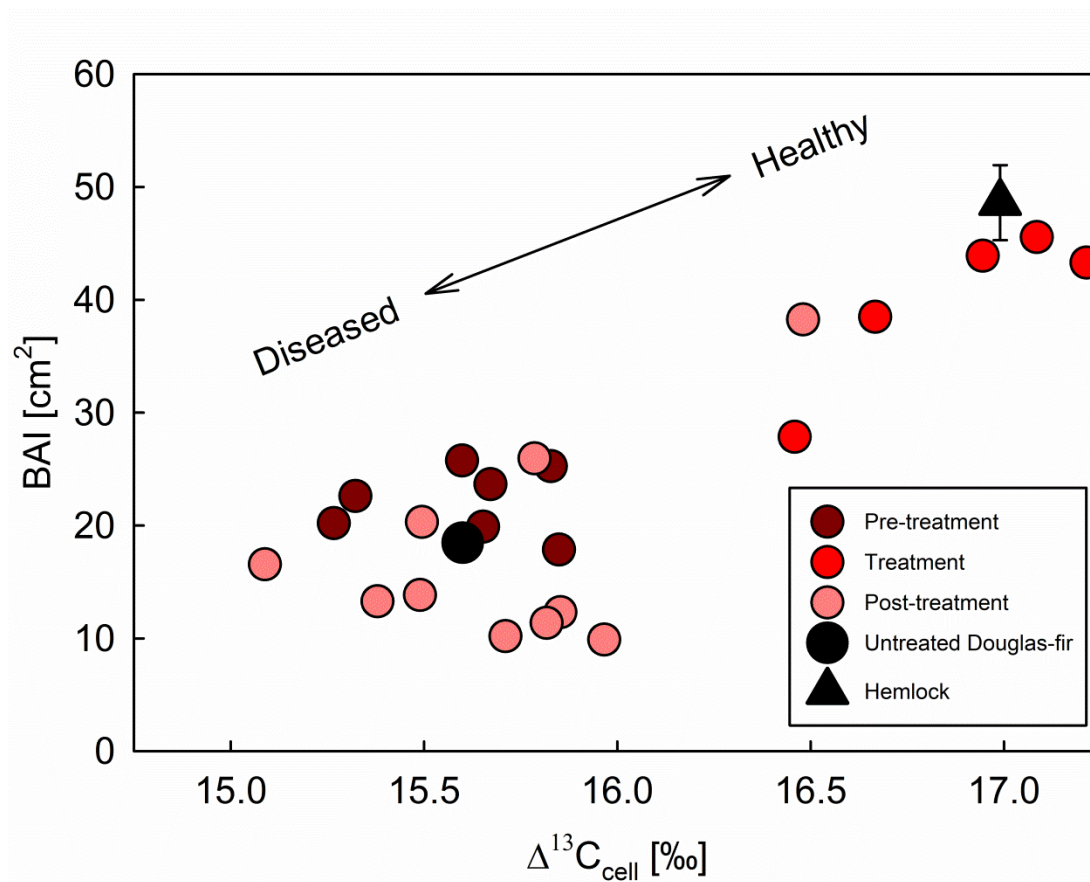


Figure 2.4 Scatterplot of mean tree-ring $\Delta^{13}C_{cell}$ and mean basal area increment (BAI) of fungicide-treated Douglas-fir post-, during, and pre-treatment (n=6 trees per treatment). Values for untreated Douglas-fir and western hemlock were averaged across all trees over the entire observation period (1989-2011) within each group. Bars represent one standard error.

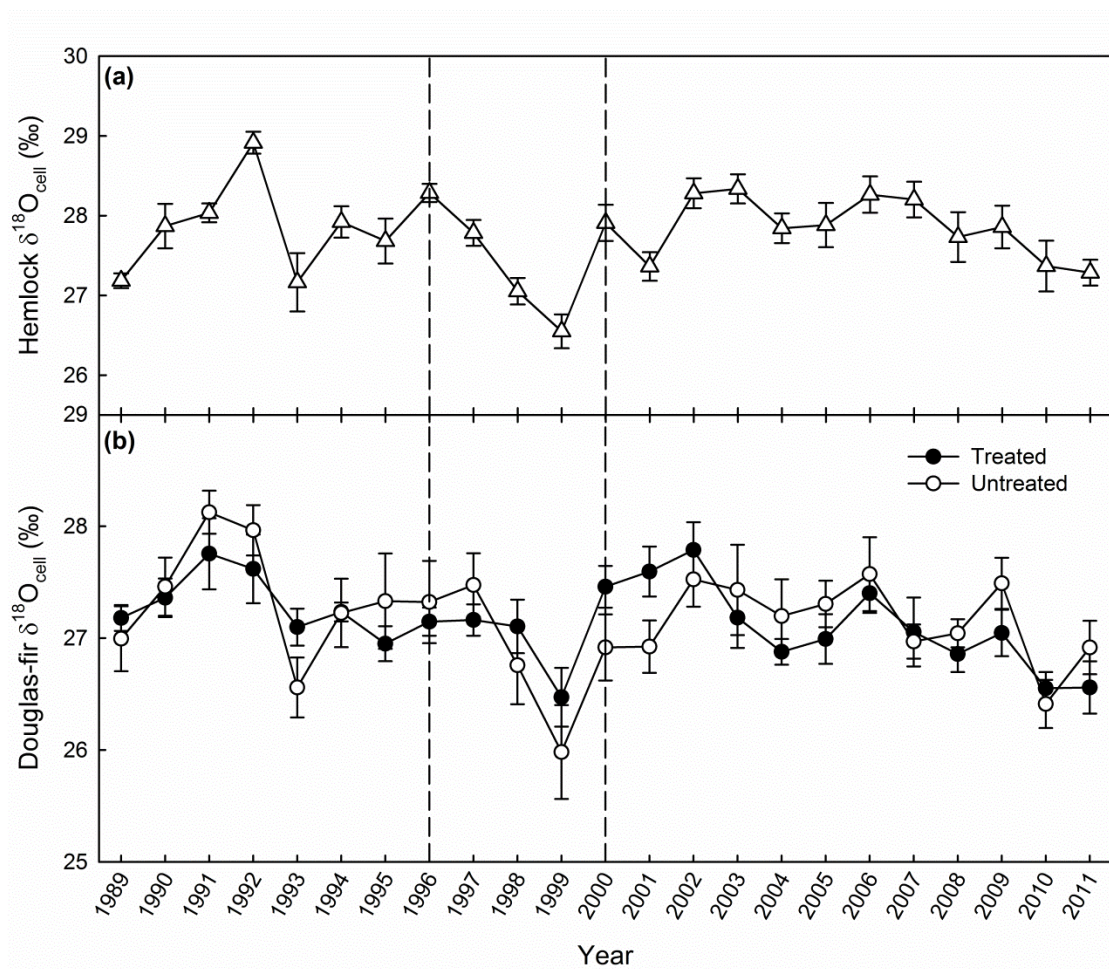


Figure 2.5 Mean tree-ring $\delta^{18}\text{O}_{\text{cell}}$ of western hemlock (a), and fungicide-treated and untreated Douglas-firs (b) at the Beaver, Oregon site during the years of observation (1989-2011; $n=6$ trees per treatment). The treatment period is indicated by vertical dashed lines (1996-2000, inclusive). Bars represent one standard error.

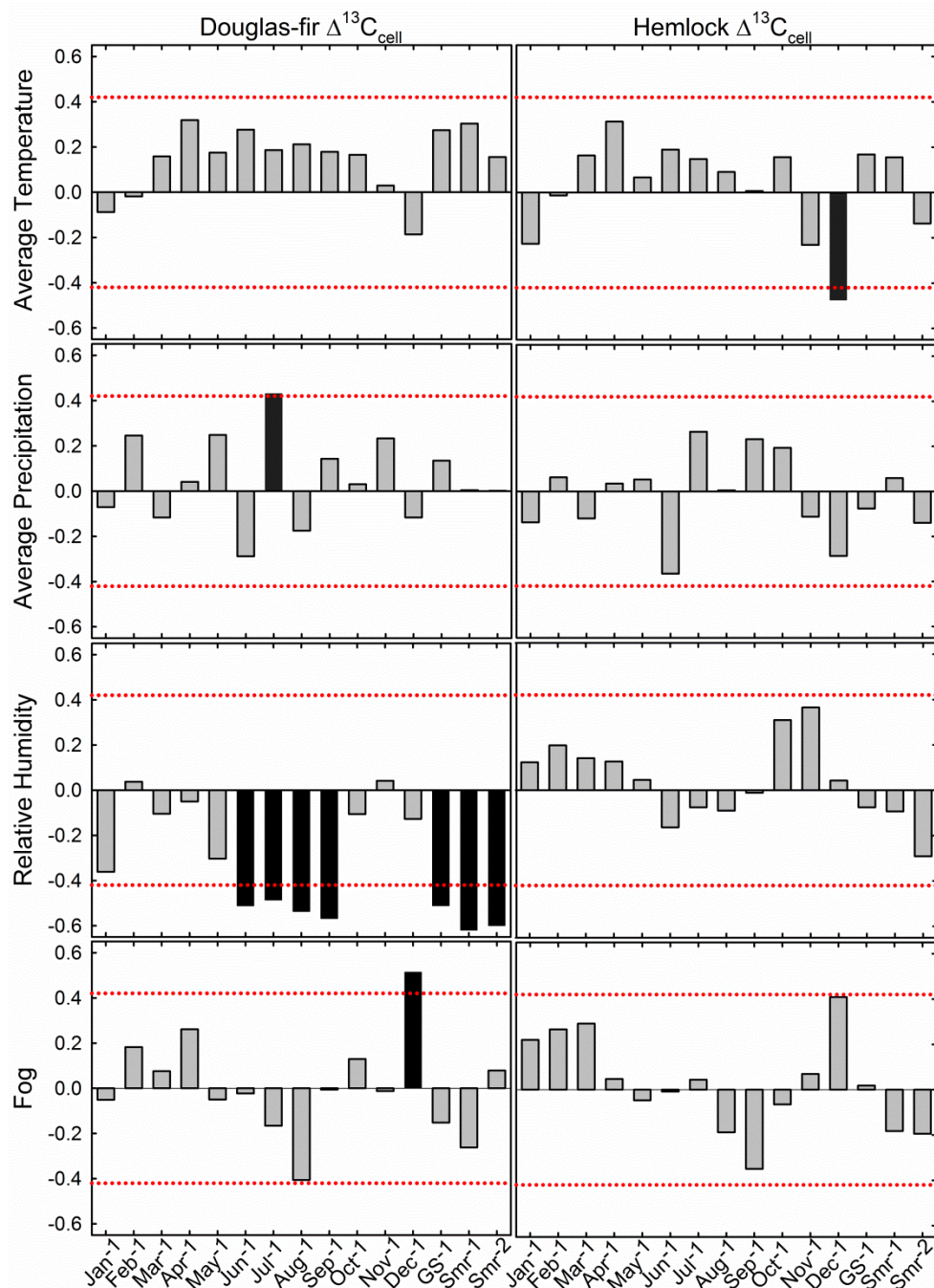


Figure 2.6 Pearson correlation coefficients (r) of Douglas-fir and western hemlock tree-ring $\Delta^{13}\text{C}_{\text{cell}}$ and various climate variables at different times of year (previous-year monthly values, previous growing season average (May-July, GS), previous summer average (June-September; Smr), and two-years-previous summer average (Smr⁻²)). Red, dotted lines represents significance at 95% confidence level (0.42/-0.42).

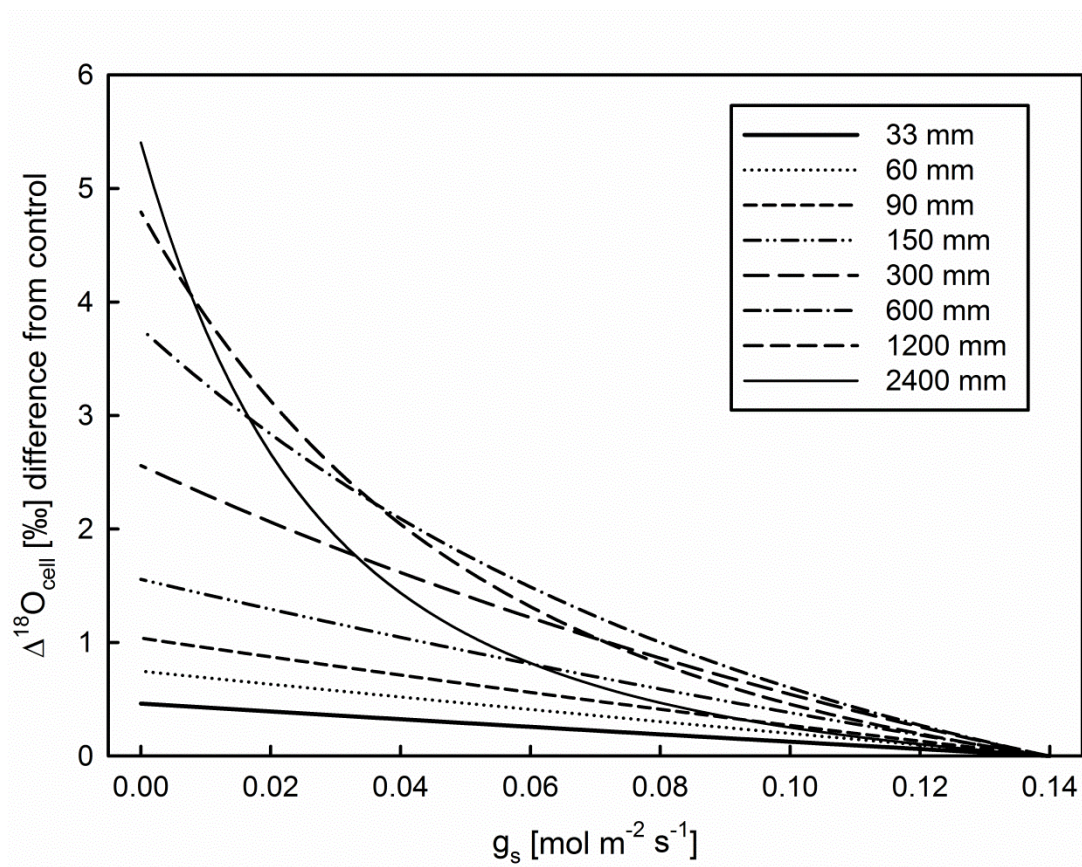


Figure 2.7 Modeled relationship between stomatal conductance (g_s) and the resulting difference in $\Delta^{18}\text{O}_{\text{cell}}$ from a control ($g_s = 0.14 \text{ mol m}^{-2} \text{ s}^{-1}$) following equations 3-6. Each line represents a different effective path length (L ; see legend).

Chapter 3

Seasonal carbohydrate dynamics and growth in Douglas-fir trees experiencing chronic, fungal-mediated reduction in functional leaf area

Abstract

Stored non-structural carbohydrate (NSC) could play an important role in tree survival in the face of a changing climate and recent trends in drought-related mortality. The effects of the stomata-blocking and defoliating fungal disease called Swiss Needle Cast (SNC) on Douglas-fir carbohydrate reserves were explored to evaluate the extent to which NSC can be mobilized under natural conditions of low water stress and restricted carbon supply in relation to potential demands for growth. Concentrations of starch, sucrose, glucose and fructose were analyzed in twig wood, foliage, and trunk sapwood of 15 Douglas-fir trees expressing a gradient of SNC symptom severity. There were significant negative relationships between disease severity and growth (mean basal area increment, BAI), as well as between disease severity and mean concentration of trunk NSC. The amount of NSC per unit growth (mean NSC/BAI), an index of the relative priority of storage versus growth, increased with disease severity in all three sampled tissues. These results suggest that under reduced carbon supply with SNC, Douglas-fir trees retain NSC at the expense of growth. The crown retains the most NSC, presumably to maintain foliage growth in the spring, which compensates for rapid foliage loss in the summer and fall.

Introduction

Recent trends in drought-related tree mortality on a global scale have led to many questions regarding the role of non-structural carbohydrate (NSC) content as an indicator of overall tree vigor and demand for photosynthate (Sala *et al.*, 2010, 2012; McDowell, 2011; Ryan, 2011; Johnson *et al.*, 2012; Wiley & Helliker, 2012). A first step towards resolving uncertainty surrounding these issues could be achieved by developing a greater understanding of the different functions that may be performed by carbohydrate reserves stored within trees.

Traditionally, NSC accumulation has been viewed as a purely passive process signifying that the supply of photosynthate exceeds demand from carbon sinks such as growth and respiratory metabolism. It is now clear that tree carbohydrate storage is multi-faceted, exhibiting patterns that suggest storage is partly passive and partly active (Chapin *et al.*, 1990; Körner, 2003; Hoch *et al.*, 2003; Würth *et al.*, 2005). Active storage is defined as a genetically-controlled process that is prioritized in carbon allocation over other carbon-dependent processes when resources are limited (Sala *et al.*, 2012). Research by Bustan *et al.* (2011) has suggested that there is an active component to storage, such that in years of heavy fruit production NSC content was not reduced in olive trees. In addition, Silpi *et al.* (2007) found that tapping rubber trees for carbon-rich latex actually caused NSC concentrations to increase.

Large carbohydrate reserves have been reported in mature trees across different climate types (Hoch *et al.*, 2003; Würth *et al.*, 2005), as well as different ecosystems and seasons (Hoch *et al.*, 2002; Körner, 2003), suggesting that trees allocate more carbon to storage than is necessary to meet normal demands (Hoch *et*

al., 2003). Furthermore, it has been observed that trees have higher than average NSC concentrations and reduced growth during prolonged periods of mild to moderate stress such as long-term water deficit (Woodruff & Meinzer, 2011a; Galvez *et al.*, 2011; Muller *et al.*, 2011) and low temperatures (Hoch & Körner, 2009). Based on current knowledge, there are a few explanations for why trees may be unable to mobilize their carbohydrate reserves for growth (Sala *et al.*, 2012). First, during periods of environmental stress such as water deficit, reduced phloem transport and cell turgor in expanding tissues would result in a constraint on sink strength resulting in reduced growth (Woodruff & Meinzer 2011b; Nikinmaa *et al.*, 2013). Because growth is more sensitive to water deficit than is photosynthesis, photosynthesis would continue despite sharply reduced allocation to growth, resulting in an accumulation of NSC (Muller *et al.*, 2011). Second, carbohydrate reserves may become sequestered and no longer available for export due to compartmentalization that restricts their propensity to be loaded into the phloem (Quick *et al.*, 1992) or impedes access of enzymes to starch (Srichuwong & Jane, 2007). Third, there may be an evolutionary advantage for trees to actively maintain a minimum level of carbohydrate reserves to support metabolism or to provide solutes for maintaining cell turgor and vascular integrity in an often stochastic and unpredictable environment, where water availability and growing conditions are not always optimal for normal plant functioning (Sala *et al.*, 2012; Wiley & Helliker, 2012).

Under conditions of water stress it is difficult to determine whether the buildup of NSC is due to passive accumulation due to reduced sink demands, sequestration, or

active storage. To better understand the role of carbon storage in tree physiology, it is necessary to determine how storage is prioritized over growth in the absence of potentially confounding factors such as those resulting from water stress. The Douglas-fir (*Pseudotsuga menziesii* (Mirb.) Franco) disease called Swiss Needle Cast (SNC) provides a unique natural experiment to examine relative priorities of growth versus carbon storage in the absence of drought-related reductions in carbon assimilation, and water and phloem transport capacity. The disease is found primarily along the Oregon coast, a region with high rainfall and a maritime climate with low risk of drought. The pathogen that causes SNC is an ascomycete (*Phaeocryptopus gaeumannii* (T. Rohde)) that colonizes Douglas-fir foliage. The spores are released in May and June, near the time of bud break for Douglas-fir, at which time they land and germinate on current-year needles (Stone *et al.*, 2008a). After a year of incubation during which the mycelia colonize the surface and inside of the needle, the mycelia may begin to produce fruiting bodies (pseudothecia) that block stomata. This blockage causes a significant decrease in stomatal conductance and photosynthesis (Manter *et al.*, 2000). Once approximately 25-30% of stomata are blocked, the needle will have reached a negative carbon balance, becomes chlorotic, and abscises from the tree (Manter *et al.*, 2000). There is a strong relationship between needle loss and the amount of pseudothecia present on foliage of trees with SNC (Manter *et al.*, 2003b), as well as between needle loss and reduced growth in diseased trees (Maguire *et al.*, 2002; Maguire *et al.*, 2011). Growth reductions can be reduced by as much as 20-50% in diseased stands (Maguire *et al.*, 2002; Johnson *et al.*, 2003; Johnson *et al.*, 2005).

The fungus does not release any toxins, nor cause any sort of known structural damage to the needle besides limiting the diffusion of carbon dioxide through the stomata and inside the needle. SNC has not yet been shown to result in tree mortality, although affected stands will live for decades under a chronic reduction in carbon supply (Maguire *et al.*, 2011).

The impact of SNC on tree carbohydrate reserves is unknown, but if NSC accumulation in Douglas-fir has an active component, then this competing sink for photosynthate would exacerbate the impact of SNC on growth and other carbon-dependent processes. SNC affords the opportunity to test for the relationship between growth, carbohydrate storage and disease symptoms because the disease involves a substantial reduction in carbon assimilation under conditions of low water stress at sites where SNC is prevalent. If NSC reserves remain largely undepleted under severe SNC, this result would provide evidence for prioritization of storage over growth, or that NSC has been sequestered. If NSC reserves become substantially depleted, this provides evidence for the ability of stored NSC to be mobilized when needed to maintain tree physiological functioning and survival. Additionally, if SNC causes a greater relative decline in growth compared to NSC reserves, this would provide evidence for storage being prioritized as carbon assimilation is reduced.

The goals of this research were: (1) to determine how SNC influences partitioning of assimilated carbon between growth and carbohydrate reserves and to determine if differences in disease severity influence relative partitioning of carbon between these two sinks; (2) to identify any seasonal differences in the impact of SNC

on partitioning of carbon between growth and reserves; and (3) to establish the extent to which carbohydrate reserves are mobilized under natural conditions of high demand for carbon and low water stress. Based on previous research, I hypothesized that relative reductions in growth of trees with SNC would be greater than relative reductions in NSC reserves and that seasonal fluctuations in NSC would be smallest in the most heavily diseased trees. Furthermore, I hypothesized that NSCs would be relatively more abundant in the crown, near the source of photosynthesis, than in the trunk as disease severity increased.

Materials and methods

Field site and sampling

A single Douglas-fir stand with a range of SNC symptom expression was selected from an Oregon Department of Forestry unit (named Prairie Hill, 45.5°N 123.8°W) located on the Oregon coast near Tillamook at approximately 134 m above sea level. The Pacific maritime climate of the region is characterized by wet winters and dry summers. Mean annual precipitation in the region is about 2.8 m. Mean annual temperature is about 10.1 °C, ranging from a mean of 5.7 °C in January to 15.3 °C in July. Although the summer from June to September is relatively dry, with a mean precipitation of about 278 mm, mean RH hovers around 80.0% and mean vapor pressure deficit (VPD) generally remains below 0.50 kPa during these months (PRISM Climate Group, <http://prism.oregonstate.edu>; data summarized from 1980 to 2011).

The stand was initially planted in 1990, with trees successively inter-planted through 1997. Trees were selected that ranged in planting date from 1990 to 1995, so the largest age difference between trees would be five years. 15 trees were non-randomly selected (Table 1), with five trees roughly fitting into each of three categories of overall needle retention (0-1.0 years, >1.0-2.0 years, >2.0+ years). Needle retention was estimated using a standard protocol in the field where the crown of each tree was visually divided into thirds and the predominant needle retention from each third was averaged (*e.g.* Maguire *et al.*, 2002; D. C. Shaw, pers. comm.).

In June, two 5 mm cores were collected to pith from opposite sides of each tree with an increment borer for annual growth measurement. The sapwood boundary was marked on each core to determine average sapwood width. Cores were stored in paper straws for transport to the laboratory. One-year-old foliage was collected from three branches located in the sun-exposed lower-mid crown of each tree to assess the presence and abundance of pseudothecia on the needles (described below).

For NSC analyses, trunk sapwood tissue was sampled with an increment borer to a depth of 2 cm at 1.3 m height on opposite sides of each tree. Foliage and twig wood were sampled from two branches located in the sun-exposed lower-mid crown of each tree. The branches were divided immediately into segments representing growth from the years 2011, 2010, and 2009 (*i.e.* one-, two-, and three-year-old tissues). Foliage was removed from the twigs, and total foliage mass (at field moisture content) was recorded for each segment from each branch and averaged for each branch, and then each tree (mean foliage mass, g). All samples (two trunk samples,

and foliage and twig samples from 2011, 2010, and 2009) were immediately placed into sealed plastic bags and onto dry ice in a cooler. Sampling was always conducted between late morning and early afternoon. In view of previous observations showing substantial seasonal variation in NSC content in Douglas-fir trees (Woodruff & Meinzer, 2011a), sampling took place three times over a seasonal cycle in 2012: around bud break (June 18), mid-summer (July 31), and late summer (September 4).

Disease severity assessment

The presence and abundance of the fungus on one-year-old foliage was determined by visual estimates of pseudothecia emerging from stomata using standard techniques (e.g. Manter *et al.*, 2005). Estimates of the percentage of stomata that were occluded with pseudothecia (*i.e.* pseudothecia counts) for each of the three branches collected in the field were calculated by averaging pseudothecia counts from three positions of 10 randomly selected needles per branch. At each position, one on each longitudinal third of the needle, pseudothecia counts were conducted by selecting a region within each position with a random number table and visually counting the number of pseudothecia emerging from 50 consecutive stomata above the needle mid-rib and 50 consecutive stomata below the needle midrib (100 stomata total in each position). The percentage of pseudothecia-occluded stomata of each needle was averaged across 10 needles per branch, and averaged again across the three branches per tree to calculate the tree pseudothecia count.

To account for the amount of functional one-year-old foliage remaining on a tree relative to its pseudothecia count, an index was created to quantify disease symptoms by multiplying the percent of non-occluded stomata ($100\% - \% \text{ occluded stomata}$) by the average one-year-old foliage dry mass per growth increment for each tree (*i.e.* functional foliage mass, g). Functional foliage mass was intentionally used as a measure of disease severity instead of the needle retention technique (described above) due to its advantages of being an integrated measure of two symptoms (pseudothecia abundance and foliage mass) and therefore more objective and precise in quantifying disease severity.

Chemical analyses

Trunk sapwood, twig wood, and foliage samples were stored in a $-20\text{ }^{\circ}\text{C}$ freezer before being microwaved for 90 s to stop all enzymatic activity, oven dried for 72 hours at $65\text{ }^{\circ}\text{C}$, and ground to a fine powder with a ball mill. The dried and ground tissue samples were analyzed for content of four components: starch, sucrose, glucose and fructose together, and total NSC following the procedure described by Woodruff and Meinzer (2011a). Deionized water was added to the samples, which were then heated in covered vials over steam for 90 min to extract NSC. After enzymatic conversion of glucose and fructose to gluconate-6-phosphate, the concentration of free glucose was determined photometrically on a 96-well microplate photometer (Multiscan FC, Thermo Scientific, Waltham, MA, USA). Samples were analyzed before and after enzymatic treatments of sucrose digestion by invertase (45 min reaction) and starch

and sucrose digestion by amyloglucosidase (15 hour reaction). Photometric analysis was based on absorbance of samples at 340 nm in solution with reference to the absorbance of a glucose reference solution. The combination of glucose and fructose content was determined from photometric analysis of sample solutions with no enzymatic treatment. Sucrose content of the samples was determined by subtracting the combination of glucose and fructose content from the glucose concentration of sample solutions following invertase enzyme treatment. Total NSC was determined from the amyloglucosidase reaction mixture, which contained the original concentrations of free glucose and fructose, plus glucose and fructose liberated from starch and sucrose. Starch content of the samples was determined by subtracting the glucose content of sample solution following invertase enzyme treatment from the total NSC content. All NSC, starch, sucrose, and glucose and fructose values for each tissue of each tree are averages of the two sampled branches collected in the field at each sampling date and are presented in units of percentage of dry weight (% dry weight).

Growth analyses

Tree-cores collected for growth analyses were air-dried, glued to wooden mounts with the transverse face upward, and sanded with progressively finer sandpaper until annual rings were distinguishable. Ring-widths were measured for each growth ring to a precision of 0.01 mm using a Velmex rotating measuring table and the program Measure J2X[®] measuring software. The cross-dating program COFECHA (Holmes,

1983; Grissino-Mayer, 2001) was used to identify possible missing and false rings.

The ring widths for the two cores from each tree were averaged and basal area increment (BAI) was calculated to characterize tree growth. The average BAI from 2000 to 2011 was calculated for each tree to represent annual tree growth (mean BAI, cm^2).

Statistical analyses

All analyses exploring the relationship between disease explanatory variables (*i.e.* pseudothecia count and functional foliage mass) and the response variables of interest (*i.e.* BAI, foliage mass, total NSC, starch, sucrose, glucose and fructose) in the trunk, twigs, and foliage were made using simple linear regression ANOVA for all 15 trees, unless otherwise noted. Assumptions of simple linear regression were checked by plotting residuals of the response variable versus fitted values to assess equality of variance and were also plotted within a normal probability plot to assess normality. Paired t-tests were performed to test for the differences in foliage mass, total NSC, starch, sucrose, and glucose and fructose from June to September for all 15 trees. Assumptions of the paired t-tests were checked by evaluating histograms of the distribution of the sample response variables.

Results

Disease severity assessment

Mean one-year-old foliage dry mass per growth increment ranged from 0.05 to 0.66 g, and pseudothecia count ranged from 5-36% stomata occluded in the 15 trees studied (Table 3.1). The maximum observed stomatal occlusion was comparable to the estimated threshold at which needle abscission would likely occur (Manter *et al.*, 2000; Table 3.1). The mean mass of one-year-old foliage (averaged across the three sampling dates) was approximately 0.26 g, whereas the mean growing season mass of three-year-old foliage was only about 0.04 g (Fig. 3.1). The mean difference in foliage mass between the two age classes was about 0.23 g (95% CI: [0.16, 0.30]). The 15 trees are ordered in Table 1 from the lowest to the highest basal area increment (BAI). There was a significant linear relationship between pseudothecia count and both mean BAI ($r^2 = 0.58$, $P = 0.0009$) and mean one-year-old foliage mass ($r^2 = 0.40$, $P = 0.01$), such that a 1% increase in pseudothecia abundance of one-year-old foliage reflected a 0.58 cm² decrease in mean BAI (95% CI: [0.29, 0.87]) and a 0.012 g decrease in mean foliage mass per growth increment (95% CI: [0.003, 0.02]). There was a very strong relationship between functional foliage mass and mean BAI ($r^2 = 0.63$, $P = 0.0004$, Fig. 3.2). The rest of the analyses described below use functional foliage mass as a measure of disease severity for each tree.

NSC and growth analyses

The relationship between NSC concentration and tissue age for twigs and foliage did not differ with disease severity (Appendix A). Thus the following analyses with

foliage and twigs only include one-year-old tissues because functional foliage mass was only evaluated for prior year foliage.

The mean concentration of NSC was approximately four to five times higher in the crown (twigs and foliage) than in the trunk across trees (Fig. 3.3). There was a significant linear relationship between functional foliage mass and mean growing season (*i.e.* averaged over the three sampling dates) trunk NSC content ($r^2 = 0.35$, $P = 0.02$), and without the outlier (tree 6), the relationship was substantially stronger ($r^2 = 0.54$, $P = 0.003$, Fig. 3.4a). Only two trees had average sapwood widths slightly less than the trunk sampling depth (*i.e.* 2 cm). Trunk NSC concentrations of these two trees were compared, along with NSC concentrations of other trees with similar sapwood widths, and no relationship between sapwood width and trunk NSC concentration was identified (data not shown). The relationship between functional foliage mass and mean trunk NSC/BAI was also significant ($r^2 = 0.53$, $P = 0.002$, Fig. 3.4b), indicating that with increasing disease severity and therefore constraints on carbon supply, the relative reduction in basal area growth was greater than that of trunk NSC storage. In contrast, there were no statistically significant relationships between functional foliage mass and mean growing season NSC content of twigs ($r^2 = 0.11$, $P = 0.23$) or foliage ($r^2 = 0.001$, $P = 0.91$, Fig. 3.5a, b). However, there were strong exponential relationships between functional foliage mass and the mean NSC/BAI for both twigs ($r^2 = 0.72$, $P = 0.0002$) and foliage ($r^2 = 0.64$, $P = 0.001$) (Fig. 3.5c, d). The trend in NSC/BAI with functional foliage mass was similar for each sampling date (data not shown).

Starch was the largest component of NSC in the trunk, followed by glucose and fructose, and then sucrose (Table 2; Fig. 3.6). In June, there was a significant linear relationship between functional foliage mass and trunk NSC content ($r^2 = 0.38$, $P = 0.02$), as well as with trunk starch content ($r^2 = 0.44$, $P = 0.007$). The positive linear relationship between functional foliage mass and trunk sucrose content was significant near the end of the growing season in July ($r^2 = 0.47$, $P = 0.004$) and September ($r^2 = 0.38$, $P = 0.01$). There was no relationship between functional foliage mass and the mean growing season trunk glucose and fructose ($r^2 = 0.04$, $P = 0.44$).

In contrast to the patterns of NSC constituents observed in trunks, each NSC component type was generally equal in relative abundance in both twigs and foliage at each sampling date (Table 3.2; Fig. 3.6). There were no significant relationships between functional foliage mass and mean growing season starch content of twigs ($r^2 = 0.18$, $P = 0.12$) or foliage ($r^2 = 0.007$, $P = 0.77$), or between functional foliage mass and mean growing season glucose and fructose content of twigs ($r^2 = 0.06$, $P = 0.38$) or foliage ($r^2 = 0.03$, $P = 0.54$). There were marginally significant relationships between functional foliage mass and mean growing season sucrose content of twigs ($r^2 = 0.23$, $P = 0.07$) and foliage ($r^2 = 0.20$, $P = 0.09$).

NSC fluctuated seasonally in all tissue types (Table 3.2; Fig. 3.6). Seasonal fluctuation was not related to functional foliage mass, such that there were no statistically significant relationships between functional foliage mass and the percent decrease in mean NSC from June to September in the trunk ($r^2 = 0.03$, $P = 0.57$), twigs ($r^2 = 0.05$, $P = 0.40$), or foliage ($r^2 = 0.0008$, $P = 0.92$). From June to September, mean

trunk NSC content decreased by 0.49% dry weight (95% CI: [0.26, 0.71]), starch content decreased by 0.47% dry weight (95% CI: [0.26, 0.68]), and sucrose content increased by 0.05% dry weight (95% CI: [0.004, 0.097]). There was no statistically significant change in mean trunk glucose and fructose over the growing season. Mean twig NSC content decreased by 2.89% dry weight from June to September (95% CI: [2.05, 3.72]) and starch content decreased by 3.23% dry weight (95% CI: [2.54, 3.93]). There was no statistically significant change in mean twig sucrose or glucose and fructose content over the growing season. Mean foliage NSC content decreased by 2.03% dry weight from June to September (95% CI: [1.03, 3.03]), foliage starch content decreased by 2.46% dry weight (95% CI: [1.58, 3.33]), and foliage sucrose content increased by 0.46% dry weight (95% CI: [0.13, 0.79]). There was no statistically significant change in mean foliage glucose and fructose over the growing season.

Discussion

The high degree of disease severity at the site was evident in the reduction in mean growing season foliage mass by about 86% from the one-year-old cohort to the three-year-old cohort (Fig. 3.1), as compared to healthier trees in the region that have been reported to show a reduction in foliage mass of about 25% over the same cohort ages (Weiskittel *et al.*, 2006). The relationships between disease severity (previous year functional foliage mass) and Douglas-fir growth and carbohydrate reserves demonstrated in this study suggest that whereas the reduction in carbon assimilation

caused by SNC results in reduced annual growth and NSC in the trunk, there is no apparent relationship between disease severity and NSC concentrations in twigs and foliage. Retaining NSC in the crown appears to have a greater priority than exporting the photosynthate for diameter growth in the trunk (Figs. 3.4 and 3.5). Thus, SNC appeared to lead to a scenario in which diseased trees were forced to sacrifice stem growth in order to maintain crown growth under conditions of rapidly abscising foliage. Carbohydrate reserves were depleted throughout the growing season to different extents in each tissue type (Table 3.2; Fig. 3.6).

A number of studies that have focused on several different conifer species growing in a variety of environments have reported fairly similar NSC concentrations and seasonal patterns. Trunk NSC in conifers is typically as high as 3% dry weight at bud burst, and as low as 0.5% dry weight at the end of the growing season (Hoch *et al.*, 2002; Hoch *et al.*, 2003; Hoch & Körner, 2003; Woodruff & Meinzer, 2011a). Starch is usually the largest component of NSC in the trunk, ranging from 65% to nearly 100% of total NSC throughout the growing season, while sucrose and glucose and fructose make up from almost none to a maximum of about 50% of total trunk NSC. NSC concentrations of foliage and twigs of conifers has been reported to be as high as 30% dry weight and to decline to as low as about 5% dry weight over the growing season, though they typically range from about 10-20% dry weight (Oleksyn *et al.*, 2000; Hoch *et al.*, 2002; Hoch *et al.*, 2003; Hoch & Körner, 2003; Bansal *et al.*, 2009; Sveinbjornsson *et al.*, 2010; Woodruff & Meinzer, 2011a). Starch is typically the largest component of NSC in the crown, usually peaking at about 80% of total

NSC in spring and reaching a low of about 50% of total NSC by the end of the growing season (Oleksyn *et al.*, 2000; Hoch *et al.*, 2002; Hoch *et al.*, 2003; Hoch & Körner, 2003; Woodruff & Meinzer, 2011a). Free sugars in conifer crowns range somewhere between 3-10% dry weight, usually with a slight to moderate increase over the growing season (Oleksyn *et al.*, 2000; Hoch *et al.*, 2002; Hoch *et al.*, 2003; Hoch & Körner, 2003; Bansal *et al.*, 2009; Woodruff & Meinzer, 2011a).

The basis for seasonal trends in NSC of conifers is fairly well studied and understood. Starch concentrations are relatively high before bud break and are drawn upon over the growing season to aid in flushing and axial growth, while free sugar concentrations (*i.e.* sucrose, glucose, and fructose) progressively increase and peak in autumn (Hoch *et al.*, 2003; Fischer & Höll, 1991; Schaberg *et al.*, 2000; Bansal *et al.*, 2009; Chung & Barnes, 1980; Kibe & Masuzawa, 1992; Oleksyn *et al.*, 2000; Hansen & Beck, 1990; Hansen & Beck, 1994). Starch is the main carbohydrate storage compound for conifers and is clearly a dynamic pool that accumulates over the winter and ensures that the tree will have a new cohort of needles for growth and metabolism during the following growing season (Webb, 1981). The accumulation of free sugars over the course of the growing season may be important in sensing xylem embolism and providing adequate concentrations of soluble sugars to reverse embolism as environmental conditions become drier throughout the summer (Bucci *et al.*, 2003; Johnson *et al.*, 2003; Secchi & Zweieniecki, 2011; Woodruff & Meinzer, 2011a) and to maintain cell turgor of parenchyma through osmotic adjustment (Koppenal *et al.*, 1991; Wang & Stutt, 1992; Millard *et al.*, 2007; Dichio *et al.*, 2009).

In this study, the trunk and crown each behaved differently in response to limited carbon availability under low environmental stress. Mean trunk NSC across trees (1.3-0.9% dry weight, June to September) was comparable to the values found in healthy trees although slightly lower than average. There was a clear decrease in trunk NSC with increasing disease symptom severity, due primarily to a decrease in starch, which represented about 45-63 % of total NSC over the growing season. In addition, there was a strong positive relationship between functional foliage mass and trunk sucrose at the end of the growing season. Thus, it appears that trunk storage (in the form of starch) was sacrificed with decreasing carbon availability, resulting in lower NSC values in more diseased trees. The higher trunk sucrose concentrations in healthier trees at the end of the growing season could be a consequence of healthier trees having more starch to mobilize at the end of the growing season for stem maintenance. The relative reduction in annual radial growth was greater than that of NSC with increasing reduction in carbon assimilation, indicating a priority of storage over growth in the trunk. This result combined with the observed lack of dependence of glucose and fructose concentrations in the trunk on carbon availability suggests that a minimum threshold of NSC was maintained due to sequestration or active retention of reserves.

In contrast, mean twig and foliage NSC was relatively low (about 6.1-3.2% and 6.5-4.5% dry weight, respectively) compared to previously reported values. The decrease in total NSC over the growing season was primarily attributable to the depletion of starch, which made up about 64% and 46% of total NSC in June and

about 22% and 12% of total NSC by September for twigs and foliage, respectively. Starch values were substantially lower at the beginning of the growing season (~ 3% dry weight of foliage) compared to reported values for mature Douglas-fir near the Oregon coast (~ 6% dry weight of foliage; Webb & Kilpatrick, 1993), while sucrose and glucose and fructose concentrations were comparable to values previously reported for Douglas-fir (Bansal *et al.*, 2009; Woodruff & Meinzer, 2011a) and other conifers (Oleksyn *et al.*, 2000; Hoch *et al.*, 2002; Hoch *et al.*, 2003; Hoch & Körner, 2003). Although disease appeared to have lowered total crown NSC across trees, there was no relationship between NSC and disease severity. Thus, it appears that under conditions of low carbon availability the crown will mobilize or sacrifice a portion of starch storage, apparent from the lower than average proportion of starch to NSC, while maintaining a certain threshold of total NSC, primarily sucrose, glucose and fructose.

Taken together, there seemed to be a greater priority to retain NSC in the crown over exporting NSC to supply diameter growth in the trunk. Figure 3.5c and d demonstrate how foliage and twig NSC/BAI ratios were much higher than those of the trunk in Figure 3.4b and increased sharply with decreasing functional foliage mass. Diseased trees appeared to be locked into a cycle of retaining a higher concentration of NSC in twigs and foliage to sustain the construction of new photosynthetic tissue and supporting branches to compensate for early needle abscission (Turgeon, 2010) at the apparent expense of greater stem growth and increased mechanical support in the trunk. This could potentially explain why trees with SNC can survive for decades

under a chronic reduction in carbon supply. Thus, the results of the present study suggest that carbon storage is either partly active and/or a portion of carbohydrate reserves are sequestered, which has implications for the understanding of the role of NSC as a passively accumulated or actively managed pool. NSC abundance in a particular tissue does not necessarily indicate that a tree is healthy or has abundant access to carbon, or even that growth is not suffering. Furthermore, the results of the present study have demonstrated how various regions of a tree behave differently in response to a reduction in carbon supply.

An increase in the priority of carbon storage over other processes like growth during periods of limited carbon supply could have implications for tree defense and interaction with biotic mortality agents. Kelsey and Manter (2004) found that trees with moderate to severe SNC had lowered wound-induced oleoresin flow, as well as less ethanol and monoterpene production, compared to healthy Douglas-fir. The authors ascribed these results to reduced availability of photosynthate since carbohydrates are an important building block of defense compounds. Furthermore, the lower sapwood moisture content in trees with more severe disease symptoms reported by Johnson *et al.* (2003) suggests that when NSC storage in the crown is prioritized over export of NSC to the trunk, the tree may be less able to reverse or prevent embolism in the trunk (Holbrook & Zwieniecki, 1999). Finally, the significant loss of carbohydrates from roots to below ground, accounting for approximately 73% of net primary productivity in coniferous temperate forests (Grier *et al.*, 1981; Fogel & Hunt, 1983), should also be affected by reduced carbon supply. There is evidence that

a reduction in carbon supply from the crown (*e.g.* from defoliation) can lead to depleted NSC reserves in roots of conifers (Webb & Karchesy, 1977; Oleksyn *et al.*, 2000). Although the effects of SNC on Douglas-fir root carbohydrate reserves are unclear, the results of the present study implying that stem NSC levels are sacrificed to maintain high concentrations in the crown suggest that roots may also have reduced NSC. Lower root NSC concentrations could have significant implications for root growth, which could restrict soil exploration and ability to obtain soil water and nutrients. Reduced NSC export might also limit root exudation, which plays a vital role in cycling of soil organic matter (Millard *et al.*, 2007) and attracting and establishing symbiotic relationships with mycorrhizae (*e.g.* Graham, 1982), which have been shown to receive approximately 30% of total assimilate from the host tree (reviewed by Soderström, 2002). Luoma and Eberhart (2006) observed that SNC-diseased Douglas-fir stands have a lower density and diversity of ectomycorrhizal fungi than that is typically found in healthy stands, suggesting that the reduction in photosynthate associated with SNC could be affecting these below-ground relationships.

Acknowledgements

This research was supported in part by NSF grant DEB-073882 and a grant from the Swiss Needle Cast Cooperative. Thank you to Alan Kanaskie and Erick Finnell for access to the site; Alena Tofte, Valerie Sims, and Horacio Paz for assistance in the

field and laboratory; and Lisa Ganio, Ariel Muldoon, and Julia Burton for statistical consulting.

Table 3.1 Individual characteristics for the sampled trees in ascending order by basal area increment (BAI).

Tree ID	Mean BAI (cm ²)*	DBH (cm)	Height (m)	Age (years)	Pseudothecia Count (%)*	Mean foliage Mass (g)*
7	3.4 (1.2)	9.1	14.0	19	36 (9)	0.05 (0.06)
1	4.8 (1.3)	10.2	17.9	20	25 (2)	0.23 (0.09)
3	4.9 (3.0)	9.9	20.1	15	27 (5)	0.25 (0.02)
5	5.0 (1.8)	11.5	14.5	20	22 (3)	0.24 (0.03)
8	5.7 (4.1)	10.5	8.7	17	17 (6)	0.19 (0.02)
13	6.7 (3.4)	12.1	15.9	14	29 (3)	0.36 (0.14)
14	6.8 (2.9)	12.7	14.7	18	23 (2)	0.18 (0.12)
10	7.6 (1.6)	14.0	15.4	20	35 (2)	0.06 (0.02)
9	9.1 (4.7)	13.5	11.0	16	22 (5)	0.36 (0.04)
2	14.1 (2.2)	18.5	23.1	20	5 (1)	0.36 (0.06)
15	16.8 (4.5)	21.5	20.6	19	22 (3)	0.66 (0.10)
4	16.8 (1.9)	18.3	23.0	17	16 (3)	0.34 (0.04)
12	17.5 (2.9)	19.1	24.1	17	13 (3)	0.50 (0.09)
11	23.3 (9.1)	21.2	18.4	21	5 (2)	0.62 (0.17)
6	26.3 (5.4)	25.8	17.9	20	9 (1)	0.36 (0.05)

* parentheses contain one standard deviation from the mean

Table 3.2 Mean concentrations (% dry weight) of total non-structural carbohydrate (NSC), starch, sucrose, and glucose and fructose (Gluc/Fruc) of the trunk, and current-year twigs and foliage of the sampled trees from each sampling date.

	Trunk				Twigs				Foliage			
	NSC (%)	Starch (%)	Sucrose (%)	Gluc/Fruc (%)	NSC (%)	Starch (%)	Sucrose (%)	Gluc/Fruc (%)	NSC (%)	Starch (%)	Sucrose (%)	Gluc/Fruc (%)
June	1.34 (0.16)	0.85 (0.13)	0.06 (0.02)	0.44 (0.05)	6.11 (0.38)	3.94 (0.35)	0.91 (0.08)	1.26 (0.11)	6.48 (0.53)	3.01 (0.43)	1.92 (0.13)	1.56 (0.10)
July	1.17 (0.13)	0.69 (0.10)	0.14 (0.02)	0.33 (0.03)	4.79 (0.34)	1.34 (0.19)	1.35 (0.12)	2.09 (0.21)	5.32 (0.30)	1.14 (0.17)	2.11 (0.09)	2.07 (0.11)
September	0.85 (0.11)	0.38 (0.07)	0.11 (0.02)	0.36 (0.04)	3.22 (0.34)	0.71 (0.19)	1.17 (0.12)	1.34 (0.11)	4.45 (0.26)	0.55 (0.10)	2.37 (0.14)	1.54 (0.11)

* Parentheses contain one standard error from the mean

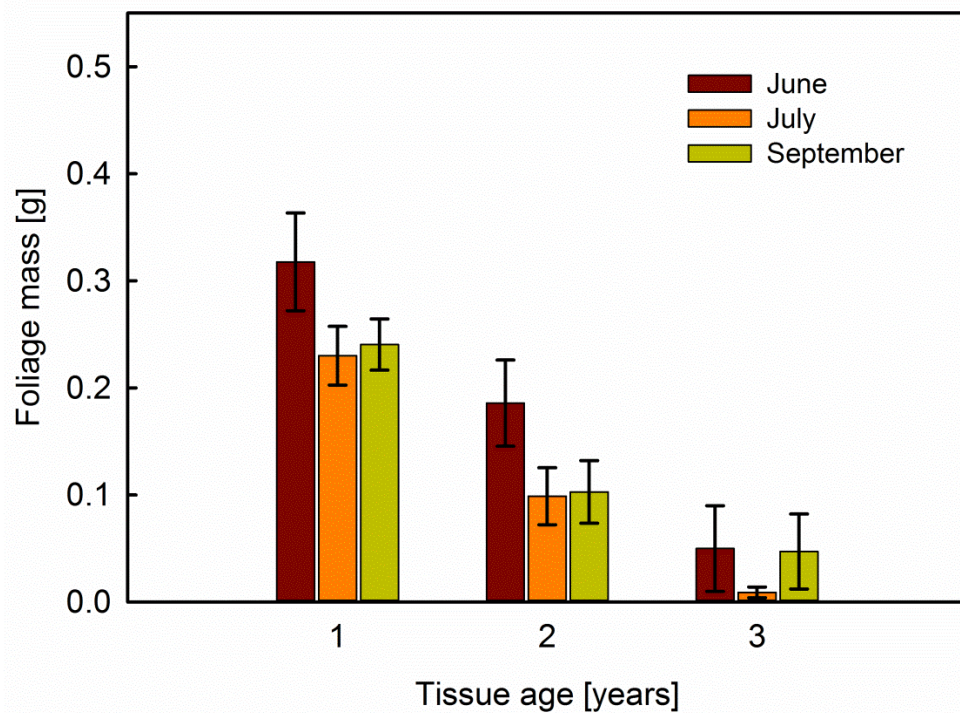


Figure 3.1 Mean foliage mass per branch growth increment for each sampled foliage tissue age at each sampling date (bars represent one standard error).

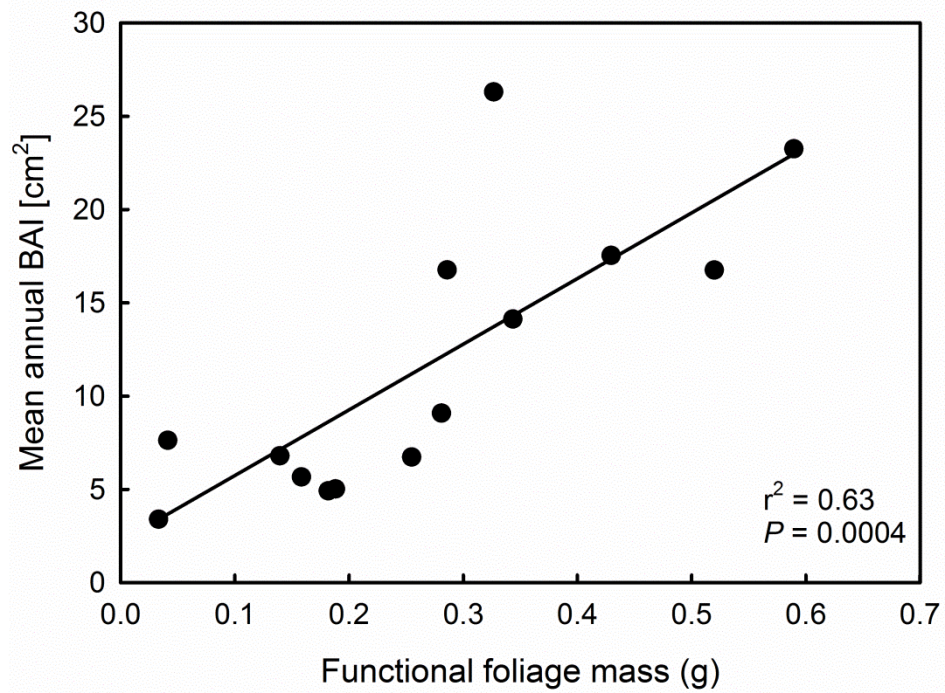


Figure 3.2 Mean annual 2000-2011 basal area increment (BAI) versus functional foliage mass with each point representing one tree and simple linear regression analysis.

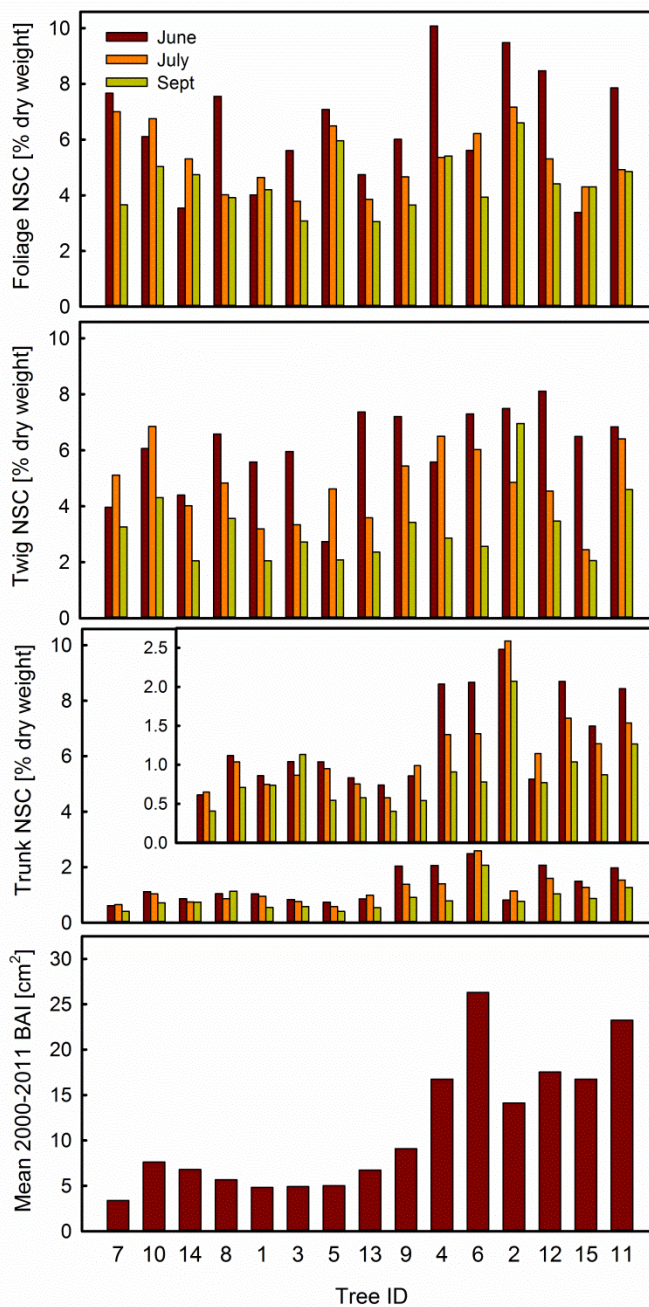


Figure 3.3 Mean non-structural carbohydrate (NSC) content for current year foliage and twigs, and trunk tissue, for each sampling date, and mean 2000-2011 basal area increment (BAI) for each sampled tree. Trees are ordered by increasing functional foliage mass. Inset in the trunk NSC panel enlarges view of trunk NSC values.

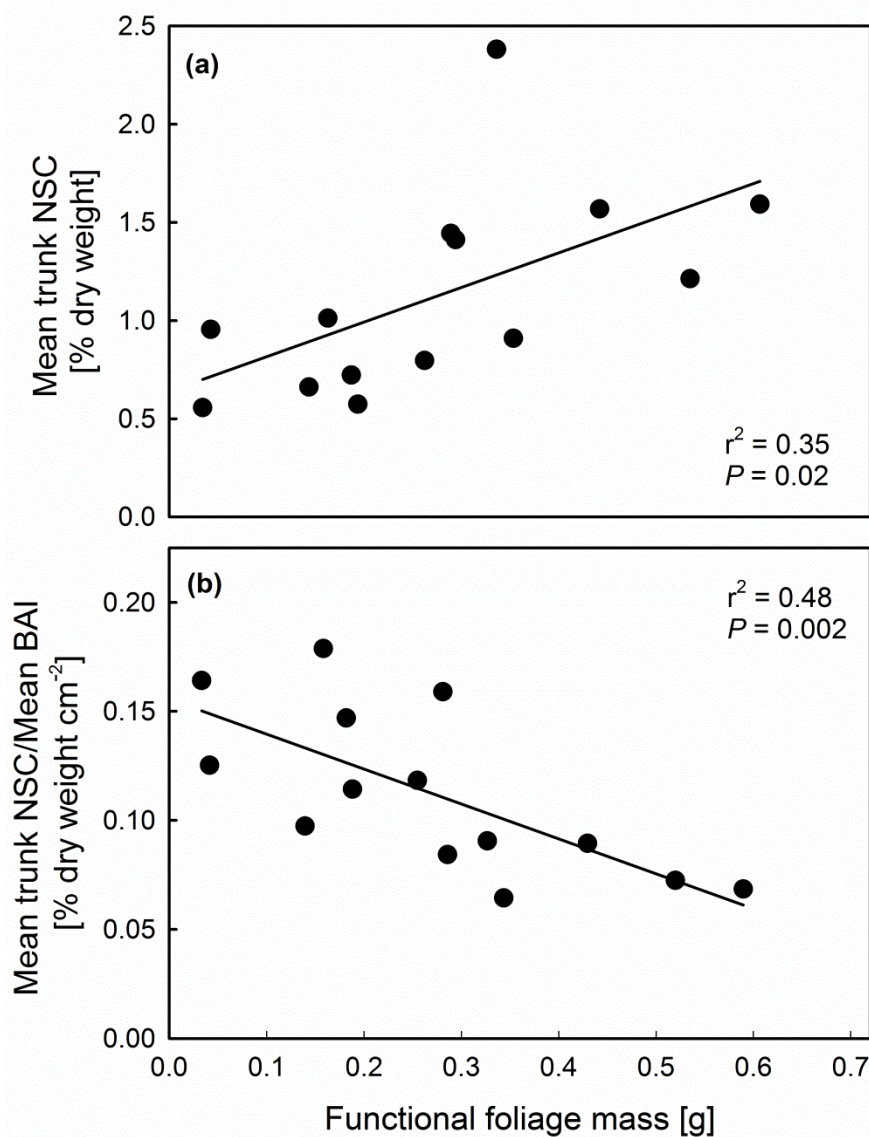


Figure 3.4 Mean trunk non-structural carbohydrate (NSC) content (a) and mean trunk NSC/ basal area increment (BAI) (b) versus functional foliage mass. Each point represents one tree. Simple linear regression analyses are shown.

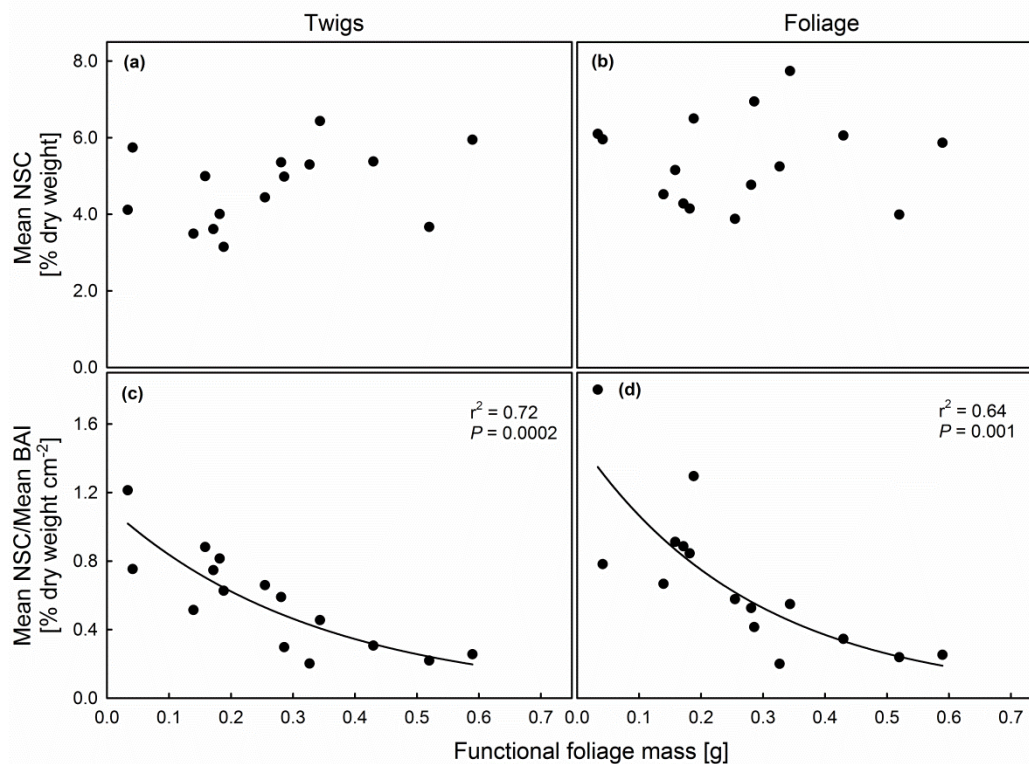


Figure 3.5 Mean twig (a) and foliage (b) non-structural carbohydrate (NSC) content and mean twig (c) and foliage (d) NSC/basal area increment (BAI) versus functional foliage mass. Each point represents one tree. Exponential decay regression analyses are shown in (c) and (d).

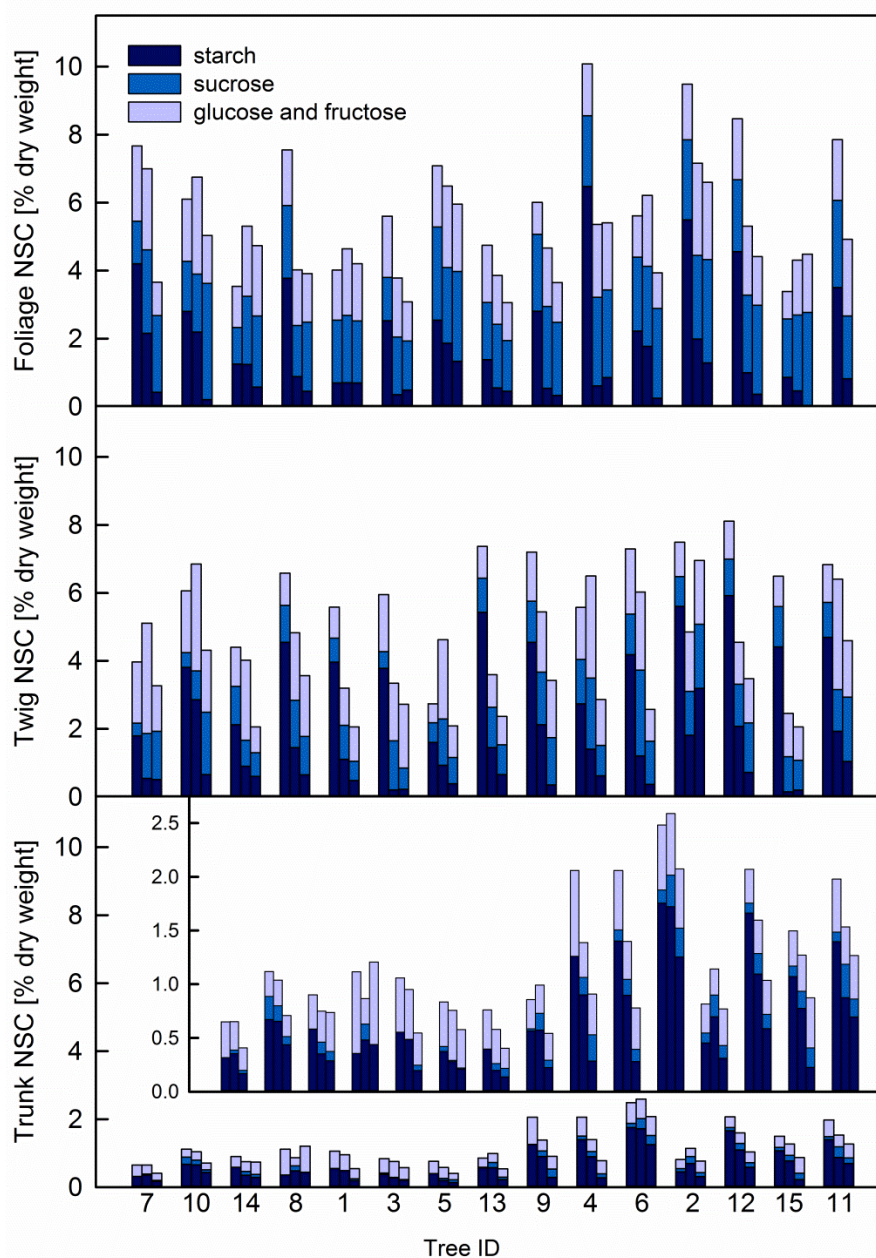


Figure 3.6 Mean foliage, twig, and trunk non-structural carbohydrate (NSC) concentrations for current year foliage and twigs, and trunk tissue, for each sampling date (ordered June, July, and September for each tree). Concentrations of NSC components (starch, sucrose, and glucose and fructose) are shown for each bar (see color legend). Trees are ordered by increasing functional foliage mass. Inset in the trunk NSC panel enlarges view of trunk NSC values.

Chapter 4

Thesis Summary

This thesis research was conducted to: (1) examine the effects of Swiss needle cast on Douglas-fir tree-ring stable isotopes of carbon and oxygen and (2) evaluate the impact of SNC disease severity on tree growth and carbohydrate reserves.

Chapter 2 describes a study that measured growth and the stable isotope values of carbon ($\Delta^{13}\text{C}$) and oxygen ($\delta^{18}\text{O}$) in Douglas-fir tree-rings to evaluate their use as proxies for variation in past SNC disease severity. The study was motivated by the hypothesis that disease-related constraints on stomatal conductance should modify the values of $\Delta^{13}\text{C}$ and $\delta^{18}\text{O}$ in fixed carbohydrates and plant tissues. Growth and tree-ring $\Delta^{13}\text{C}$ of Douglas-fir without disease was significantly greater than that of Douglas-fir with disease. In addition, evidence of the effect of disease on $\Delta^{13}\text{C}$ in the crown was found, such that older foliage with higher fungal abundance and the attached twigs had lower $\Delta^{13}\text{C}$ values. Annual growth and tree-ring $\Delta^{13}\text{C}$ of Douglas-fir without disease had values similar to co-occurring western hemlock. The use of $\Delta^{13}\text{C}$ in Douglas-fir tree-rings may be a practical approach to tracking SNC disease history provided that a co-occurring, reference species that is not susceptible to SNC disease is available to develop a parallel $\Delta^{13}\text{C}$ chronology. There was no difference in tree-ring $\delta^{18}\text{O}$ between Douglas-fir with and without disease. A modeling exercise using the models presented by Farquhar and Lloyd (1993) and Barbour and Farquhar (2000) (Chapter 2: Equations 3 and 6, respectively) demonstrated that high RH at the sampling site may

have masked any effect of differences in stomatal conductance and transpiration on tree-ring $\delta^{18}\text{O}$ in trees with and without disease. Tree-ring $\Delta^{13}\text{C}$ of diseased Douglas-fir was negatively correlated with previous summer RH, consistent with increased disease severity under high humidity. This result is likely a reflection of the facilitative effects of increased leaf wetness on fungal abundance, and thus disease severity, in the following year (Hansen *et al.*, 2000; Rosso & Hansen, 2003).

Chapter 3 describes a study in which relationships between SNC and Douglas-fir carbohydrate reserves and growth were evaluated. The purpose of this study was to determine the extent to which non-structural carbohydrate (NSC) can be mobilized under natural conditions of low water stress (since SNC is primarily found in regions of the Pacific Northwest that are not water-limited), and to examine disease-related restrictions in carbon supply in relation to potential demands for growth. Annual growth was measured from tree-rings, and concentrations of starch, sucrose, glucose and fructose were analyzed in twig wood, foliage, and trunk sapwood of 15 Douglas-fir trees expressing a gradient of SNC symptom severity. There were significant negative relationships between disease severity (measured as functional foliage mass) and growth ($r^2 = 0.63$; mean basal area increment, BAI), as well as between disease severity and mean concentration of trunk NSC ($r^2 = 0.35$, $r^2 = 0.54$ without outlier). There were no significant relationships between disease severity and the mean concentration of twig wood and foliage NSC. The amount of NSC per unit growth (mean NSC/BAI), an index of the relative priority of storage versus growth, increased with disease severity in the trunk, twigs, and foliage ($r^2 = 0.53$, $r^2 = 0.72$, $r^2 = 0.64$,

respectively). The results of this study suggest that under a reduced carbon supply, Douglas-fir trees with SNC retain NSC at the expense of growth. NSC concentrations were highest in the crown, seemingly to maintain foliage growth in the spring to compensate for rapid foliage loss in the summer and fall, which could potentially explain why trees with SNC can survive for decades under a chronic reduction in carbon supply. Furthermore, the results of this study suggest that carbohydrate storage may occur at the expense of maintaining other metabolic processes beyond trunk growth, such as the production of defense compounds and the maintenance of beneficial below-ground relationships with mycorrhizae. With regard to the implications of the present study for research in drought-related tree mortality, the results suggest that carbon storage is either partly active and/or a portion of carbohydrate reserves are sequestered, which has implications for the understanding of the role of NSC as a passively accumulated or actively managed pool.

Due to the grand spatial extent of SNC in the Pacific Northwest and its considerable effects on the productivity of an economically important timber species, Douglas-fir, this disease certainly merits attention and consideration from land managers and forest scientists. Understanding the mechanisms of disease in forest pathology is a critical component to learning how to most efficiently manage tree diseases like SNC. This thesis research has provided two important and timely contributions to the greater understanding of the pathophysiology of SNC on Douglas-fir that should ultimately inform management decisions in Pacific Northwest forests affected by SNC.

Bibliography

- Agrios GN. 2005.** *Plant pathology*. San Diego, USA: Academic Press.
- Bansal S, Germino MJ. 2009.** Temporal variation of nonstructural carbohydrates in montane conifers: similarities and differences among developmental stages, species and environmental conditions. *Tree Physiology* **29**: 559-568.
- Barbour MM, Farquhar GD. 2000.** Relative humidity- and ABA-induced variation in carbon and oxygen isotope ratios of cotton leaves. *Plant, Cell & Environment* **23**: 473-485.
- Barbour MM. 2007.** Stable oxygen isotope composition of plant tissue: a review. *Functional Plant Biology* **34**: 83-94.
- Barbour MM, Warren CR, Farquhar GD, Forrester G, Hamish B. 2010.** Variability in mesophyll conductance between barley genotypes, and effects on transpiration efficiency and carbon isotope discrimination. *Plant, Cell & Environment* **33**: 1176-1185.
- Barnard HR, Brooks JR, Bond BJ. 2012.** Applying the dual-isotope conceptual model to interpret physiological trends under uncontrolled conditions. *Tree Physiology* **32**: 1183-1198.
- Barnard RL, Salmon Y, Kodama N, Sörgel K, Holst J, Rennenberg H, Gessler A, Buchmann N. 2007.** Evaporative enrichment and time lags between $\delta^{18}\text{O}$ of leaf water and organic pools in a pine stand. *Plant, Cell & Environment* **30**: 539-550.
- Black BA, Shaw DC, Stone JK. 2010.** Impacts of Swiss needle cast on overstory Douglas-fir forests of the western Oregon coast range. *Forest Ecology and Management* **259**: 1673-1680.
- Bond BJ, Kavanagh KL. 1999.** Stomatal behavior of four woody species in relation to leaf-specific hydraulic conductance and threshold water potential. *Tree Physiology* **19**: 503-510.
- Boyce JS. 1940.** A needle cast of Douglas-fir associated with *Adelopus gaeumannii*. *Phytopathology* **30**: 649-659.
- Brooks JR, Mitchell AK. 2011.** Interpreting tree response to thinning and fertilization using tree-ring stable isotopes. *New Phytologist* **190**: 770-782.

- Brown AV, Rose DR, Webber JF. 2003.** Red band needle blight of pine. Forest Research Information Note 49. Forestry Commission, Edinburgh, UK.
- Bucci SJ, Scholz FG, Goldstein G, Meinzer FC, Da L, Sternberg SL. 2003.** Dynamic changes in hydraulic conductivity in petioles of two savanna tree species: factors and mechanisms contributing to the refilling of embolized vessels. *Plant, Cell & Environment* **26**: 1633-1645.
- Bustan A, Avni A, Lavee S, Zipori I, Yeselson Y, Schaffer AA, Riov J, Dag A. 2011.** Role of carbohydrate reserves in yield production of intensively cultivated oil olive (*Olea europaea* L.) trees. *Tree Physiology* **31**: 519-530.
- Capitano B. 1999.** *The infection and colonization of Douglas-fir by P. gaeumannii*. MSc thesis, Oregon State University, Corvallis, OR, USA.
- Cermak J, Kucera J, Bauerle WL, Phillips N, Hinckley TM. 2007.** Tree water storage and its diurnal dynamics related to sap flow and changes in stem volume in old-growth Douglas-fir trees. *Tree Physiology* **27**: 181-198.
- Cernusak LA, Tcherkez G, Keitel C, Cornwell WK, Santiago LS, Knohl A, Barbour MM, Williams DG, Reich PB, Ellsworth DS et al. 2009.** Why are non-photosynthetic tissues generally ^{13}C enriched compared with leaves in C_3 plants? Review and synthesis of current hypotheses. *Functional Plant Biology* **36**: 199-213.
- Chabot BF, Hicks DJ. 1982.** The ecology of leaf life spans. *Annual Review of Ecology and Systematics* **13**: 229-259.
- Chapin FS III, Schulze ED, Mooney HA. 1990.** The ecology and economics of storage in plants. *Annual Review Ecology and Systematics* **21**: 423-427.
- Chastagner GA, Byther RS. 1983.** Infection period of *Phaeocryptopus gaeumannii* on Douglas-fir needles in western Washington. *Plant Disease* **67**: 811-813.
- Chen ZC. 1972.** *Adelopus* [*Phaeocryptopus gaeumannii*] needle cast disease of Douglas-fir in central New York. *Taipei National Taiwan University Forest Experimental Station Technical Bulletin* **103**: 51.
- Chung HH, Barnes RL. 1980.** Photosynthate allocation in *Pinus taeda*. II. Seasonal aspects of photosynthate allocation to different biochemical fractions in shoots. *Canadian Journal of Forest Research* **10**: 338-347.

- Cook ER, Krusic PJ. 2005.** ARSTAN user's guide: A tree-ring standardization program based on detrending and autoregressive time series modeling, with interactive graphics. Lamont Doherty Earth Observatory, Columbia University, Palisades, NY, USA.
- Coop L, Stone JK. 2007.** Prediction maps of Swiss needle cast needle retention based on climatic factors. In: Shaw DC, ed. *Swiss Needle Cast Cooperative Annual Report 2007*, 15-21.
- Craig H, Gordon LI. 1965.** Deuterium and oxygen 18 variations in the ocean and the marine atmosphere. In: Tongiorgi E, ed. *Proceedings of a conference on stable isotopes in oceanographic studies and paleotemperatures, Spoleto, Italy*, 9-130.
- de Kort I. 1993.** Relationships between sapwood amount, latewood percentage, moisture content and crown vitality of Douglas-fir, *Pseudotsuga menziesii*. *International Association of Wood Anatomists Journal* **14**: 413-427.
- Dichio B, Margiotta G, Xiloyannis C, Bufo SA, Sofo A, Cataldi TRI. 2009.** Changes in water status and osmolyte contents in leaves and roots of olive plants (*Olea europaea* L.) subjected to water deficit. *Trees* **23**: 247-256.
- Domec JC, Gartner BL. 2002.** How do water transport and water storage differ in coniferous earlywood and latewood? *Journal of Experimental Botany* **53**: 2369-2379.
- Dongmann G, Nurnberg HW, Forstel H, Wagener K. 1974.** On the enrichment of H²18O in the leaves of transpiring plants. *Radiation and Environmental Biophysics* **11**: 41-52.
- Edmonds RL, Agee JK, Gara RI. 2011.** *Forest health and protection*. Long Grove, USA: Waveland Press, Inc.
- Edwards WRN, Jarvis PG. 1982.** Relations between water content, potential and permeability in stems of conifers. *Plant, Cell & Environment* **5**: 271-277.
- Ewers FW, Schmid R. 1981.** Longevity of needle fascicles of *Pinus longaeva* (bristlecone pine) and other North American pines. *Oecologia* **51**: 107-115.
- Farquhar GD, O'Leary MH, Berry JA. 1982.** On the relationship between carbon isotope discrimination and the intercellular carbon dioxide concentration in leaves. *Australian Journal of Plant Physiology* **9**: 121-137.

- Farquhar GD, Richards RA. 1984.** Isotopic composition of plant carbon correlates with water-use efficiency of wheat genotypes. *Australian Journal of Plant Physiology* **11**: 539-552.
- Farquhar GD, Hubrick KT, Condon AG, Richards RA. 1989.** Carbon isotope fractionation and plant water-use-efficiency. In: Rundel PA, Ehrlinger JR, Nagy KH, eds. *Stable isotopes in ecological research*. Berlin, DE: Springer-Verlag, 21-40.
- Farquhar GD, Lloyd J. 1993.** Carbon and oxygen isotope effects in the exchange of carbon dioxide between terrestrial plants and the atmosphere. In: Ehrlinger JR, Hall AE, Farquhar GD, eds. *Stable isotopes and plant carbon-water relations*. San Diego, USA: Academic Press, 47-70.
- Farquhar GD, Cernusak LA. 2005.** On the isotopic composition of leaf water in the non-steady state. *Functional Plant Biology* **32**: 293-303.
- Flexas J, Ribas-Carbó M, Diaz-Espejo A, Galmés J, Medrano H. 2008.** Mesophyll conductance to CO₂: current knowledge and future prospects. *Plant, Cell & Environment* **31**: 602-621.
- Flexas J, Barbour MM, Brendel O, Cabrera HM, Carriquí M, Diaz-Espejo A, Douthe C, Dreyer E, Ferrio JP, Galle A et al. 2012.** Mesophyll diffusion conductance to CO₂: an unappreciated central player in photosynthesis. *Plant Science* **193-194**: 70-84.
- Fischer C, Höll W. 1991.** Food reserves of Scots pine (*Pinus sylvestris* L.). I. Season changes in the carbohydrate and fat reserves of pine needles. *Trees* **5**: 187-195.
- Fogel R, Hunt G. 1983.** Contribution of mycorrhizae and soil fungi to nutrient cycling in a Douglas-fir ecosystem. *Canadian Journal of Forest Research* **13**: 219-232.
- Ford KF, Morton HL. 1971.** Etiology, impact, and distribution of Swiss needle cast of Douglas-fir in Michigan. *Phytopathology* **61**: 1023.
- Galvez DA, Landhäusser SM, Tyree MT. 2011.** Root carbon reserve dynamics in aspen seedlings: does simulated drought induce reserve limitation? *Tree Physiology* **31**: 250-257.
- Glawe DA. 2008.** The powdery mildews: a review of the world's most familiar (yet poorly known) plant pathogens. *Annual Review of Phytopathology* **46**: 27-51.

- Gordon TR, Duniway JM. 1982.** Effects of powdery mildew infection on the efficiency of CO₂ fixation and light utilization of sugar beet leaves. *Plant Physiology* **69**: 139-142.
- Graham JH. 1982.** Effect of citrus root exudates on germination of chlamydozoospores of the vesicular-arbuscular mycorrhizal fungus, *Glomus epigaeum*. *Mycologia* **74**: 831-835.
- Granier A, Biron P, Lemoine D. 2000.** Water balance, transpiration and canopy conductance in two beech stands. *Agricultural and Forest Meteorology* **100**: 291-308.
- Grier CC, Vogt KA, Keyes MR, Edmonds RL. 1981.** Biomass distribution and above- and below-ground production in young and mature *Abies amabilis* zone ecosystems of the Washington Cascades. *Canadian Journal of Forest Research* **11**: 155-167.
- Grissino-Mayer HD. 2001.** Evaluating crossdating accuracy: a manual and tutorial for the computer program COFECHA. *Tree-Ring Research* **57**: 205-221.
- Hansen EM, Lewis KJ. 1997.** *Compendium of conifer diseases*. St. Paul, USA: APS Press.
- Hansen EM, Stone JK, Capitano BR, Rosso P, Sutton W, Winton L, Kanaskie A, McWilliams MG. 2000.** Incidence and impact of Swiss needle cast in forest plantations of Douglas-fir in coastal Oregon. *Plant Disease* **84**: 773-778.
- Hansen J, Beck E. 1990.** The fate and path of assimilation products in the stem of 8-year-old Scots pine (*Pinus sylvestris* L.) trees. *Trees* **4**: 16-21.
- Hansen J, Beck E. 1994.** Seasonal changes in the utilization and turnover of assimilation products in 8-year-old Scots pine (*Pinus sylvestris* L.) trees. *Trees* **8**: 172-182.
- Harry DE, Kimmerer TW. 1991.** Molecular genetics and physiology of alcohol dehydrogenase in woody plants. *Forest Ecology and Management* **43**: 251-272.
- Hoch G, Popp M, Körner C. 2002.** Altitudinal increase of mobile carbon pools in *Pinus cembra* suggests sink limitation of growth at the Swiss treeline. *Oikos* **98**: 361-374.

- Hoch G, Körner C. 2003.** The carbon charging of pines at the climatic treeline: a global comparison. *Oecologia* **135**: 10-21.
- Hoch G, Richter A, Körner C. 2003.** Non-structural carbon compounds in temperate forest trees. *Plant, Cell & Environment* **26**: 1067-1081.
- Hoch G, Körner C. 2009.** Growth and carbon relations of tree line forming conifers at constant vs. variable low temperatures. *Journal of Ecology* **97**: 57-66.
- Holbrook NM, Zwieniecki MA. 1999.** Embolism repair and xylem tension: do we need a miracle. *Plant Physiology* **120**: 7-10.
- Holmes RL. 1983.** Computer assisted quality control in tree-ring dating and measurement. *Tree-Ring Bulletin* **43**: 69-78.
- Honegger R. 1986.** Haustorial types and their frequencies in a range of lichens with trebouxiod photobionts. *New Phytologist* **103**: 785-795.
- Hood IA. 1982.** *Phaeocryptopus gaeumannii* on *Pseudotsuga menziesii* in Southern British Columbia. *New Zealand Journal of Forest Science* **12**: 415-424.
- Hood IA, Kershaw DJ. 1975.** Distribution and infection period of *Phaeocryptopus gaeumannii* in New Zealand. *New Zealand Journal of Forest Science* **5**: 201-208.
- Hubbard RM, Ryan MG, Stiller V, Sperry JS. 2001.** Stomatal conductance and photosynthesis vary linearly with plant hydraulic conductance in ponderosa pine. *Plant, Cell & Environment* **24**: 113-121.
- Iwasa Y, Kobu T. 1997.** Optimal size of storage for recovery after unpredictable disturbances. *Evolutionary Ecology* **11**: 41-65.
- Johnson DM, McCulloh KA, Woodruff DR, Meinzer FC. 2012.** Hydraulic safety margins and embolism reversal in stems and leaves: why are conifers and angiosperms so different? *Plant Science* **195**: 48-53.
- Johnson GR, Gartner BL, Maguire D, Kanaskie A. 2003.** Influence of Bravo fungicide applications on wood density and moisture content of Swiss needle cast affected Douglas-fir trees. *Forest Ecology and Management* **186**: 339-348.

- Johnson GM, Grotta AT, Gartner BL, Downes G. 2005.** Impact of the foliar pathogen Swiss needle cast on wood quality of Douglas-fir. *Canadian Journal of Forest Research* **35**: 331-339.
- Johnstone JA, Dawson TE. 2010.** Climatic context and ecological implications of summer fog decline in the coast redwood region. *Proceedings of the National Academy of Sciences* **107**: 4533-4538.
- Kanaskie A, McWilliams M. 2010.** Swiss needle cast aerial survey, 2010. In: Shaw DC, ed. *Swiss Needle Cast Cooperative Annual Report 2010*, 7-10.
- Kelsey RG, Joseph G. 1998.** Ethanol in Douglas-fir with black-stain root disease (*Leptographium wageneri*). *Canadian Journal of Forest Research* **28**: 1207-1212.
- Kelsey RG, Manter DK. 2004.** Effect of Swiss needle cast on Douglas-fir stem ethanol and monoterpene concentrations, oleoresin flow, and host selection by the Douglas-fir beetle. *Forest Ecology and Management* **190**: 241-253.
- Kibe T, Masuzawa T. 1992.** Seasonal changes in the amount of carbohydrates and photosynthetic activity of *Pinus pumila* Regel on alpine in central Japan. *Proceedings of the NIPR Symposium of Polar Biology* **5**: 118-124.
- Koppenal RS, Tschaplinski TJ, Colombo SJ. 1991.** Carbohydrate accumulation and turgor maintenance in seedling shoots and roots of two boreal conifers subjected to water stress. *Canadian Journal of Botany* **69**: 2522-2528.
- Körner C. 2003.** Carbon limitation in trees. *Journal of Ecology* **91**: 4-17.
- Lai CT, Ehleringer JR, Bond BJ, U KTP. 2006.** Contributions of evaporation, isotopic non-steady state transpiration and atmospheric mixing on the $\delta^{18}\text{O}$ of water vapour in Pacific Northwest coniferous forests. *Plant, Cell & Environment* **29**: 77-94.
- Latta G, Adams D, Shaw DC. 2009.** Mapping western Oregon Douglas-fir foliage retention with a simultaneous autoregressive model. In: Shaw DC, Woolley T, eds. *Swiss Needle Cast Cooperative Annual Report 2009*, 37-51.
- Leavitt SW, Danzer SR. 1993.** Methods for batch processing small wood samples to holocellulose for stable-carbon isotope analysis. *Analytical Chemistry* **65**: 87-89.

- Luoma DL, Eberhart JL. 2006.** Are differences in the ectomycorrhizal community correlated with Swiss needle cast severity? In: Shaw DC, ed. *Swiss Needle Cast Cooperative Annual Report 2006*, 60-64.
- Maguire DA, Kanaskie A, Voelker W, Johnson R, Johnson G. 2002.** Growth of young Douglas-fir plantations across a gradient in Swiss needle cast severity. *Western Journal of Applied Forestry* **17**: 86-95.
- Maguire DA, Mainwaring DB, Kanaskie A. 2011.** Ten-year growth and mortality in young Douglas-fir stands experiencing a range in Swiss needle cast severity. *Canadian Journal of Forest Research* **41**: 2064-2076.
- Mainwaring DB, Maguire DA, Kanaskie A, Brandt J. 2005.** Growth response to commercial thinning in Douglas-fir stands with varying intensity of Swiss needle cast. *Canadian Journal of Forest Research* **35**: 2394-2402.
- Manion PD. 1991.** *Tree disease concepts*. Upper Saddle River, USA: Prentice Hall.
- Manter DK. 2000.** *Physiological impacts of Swiss needle cast*. PhD thesis, Oregon State University, Corvallis, OR, USA.
- Manter DK, Bond BJ, Kavanagh KL, Rosso PH, Filip GM. 2000.** Pseudothecia of Swiss needle cast fungus, *Phaeocryptopus gaeumannii*, physically block stomata of Douglas-fir, reducing CO₂ assimilation. *New Phytologist* **148**: 481-491.
- Manter DK. 2002.** Energy dissipation and photoinhibition in Douglas-fir needles with a fungal-mediated reduction in photosynthetic rates. *Phytopathology* **150**: 674-679.
- Manter DK, Bond BJ, Kavanagh KL, Stone JK, Filip GM. 2003a.** Modelling the impacts of the foliar pathogen, *Phaeocryptopus gaeumannii*, on Douglas-fir physiology: Net canopy carbon assimilation, needle abscission, and growth. *Ecological Modelling* **164**: 211-226.
- Manter DK, Winton LM, Filip GM, Stone JK. 2003b.** Assessment of Swiss needle cast disease: temporal and spatial investigations of fungal colonization and symptom severity. *Journal of Phytopathology* **151**: 344-351.
- Manter NK, Kavanagh KL. 2003.** Stomatal regulation in Douglas-fir following a fungal-mediated chronic reduction on leaf area. *Trees* **17**: 485-491.

- Manter DK, Reeser PW, Stone JK. 2005.** A climate-based model for predicting geographic variation in Swiss needle cast severity in the Oregon coast range. *Phytopathology* **95**: 1256-1265.
- Marschener H. 1995.** *Mineral nutrition of higher plants*. London, UK: Academic Press.
- McCarroll D, Loader NJ. 2004.** Stable isotopes in tree-rings. *Quaternary Science Reviews* **23**: 771-801.
- McDowell NG. 2011.** Mechanisms linking drought, of hydraulics, carbon metabolism, and vegetation mortality. *Plant Physiology* **155**: 1051-1059.
- Michaels E, Chastagner GA. 1984.** Seasonal availability of *Phaeocryptopus gaeumannii* ascospores and conditions that influence their release. *Plant Disease* **68**: 942-944.
- Millard P, Sommerkorn M, Grelet GA. 2007.** Environmental change and carbon limitation in trees: a biochemical, ecophysiological and ecosystem appraisal. *New Phytologist* **175**: 11-28.
- Muller B, Pantin F, Génard M, Turc O, Freixes S, Piques M, Gibon Y. 2011.** Water deficits uncouple growth from photosynthesis, increase C content, and modify the relationship between C and growth in sink organs. *Journal of Experimental Botany* **62**: 1715-1729.
- Nikinmaa E, Hölttä T, Hari P, Kolari P, Mäkelä A, Sevanto S, Vesala T. 2013.** Assimilate transport in phloem sets conditions for leaf gas exchange. *Plant, Cell & Environment* **36**: 655-669.
- O'Leary M. 1988.** Carbon Isotope in Photosynthesis. *BioScience* **38**: 328-336.
- Oleksyn J, Zytkowski R, Karolewski P, Reich PB, Tjoelker MG. 2000.** Genetic and environmental control of seasonal carbohydrate dynamics in trees of diverse *Pinus sylvestris* populations. *Tree Physiology* **20**: 837-847.
- Onaka F. 1950.** The longitudinal distribution of radial increments in trees. *Bulletin of the Kyoto University Forests* **18**: 1-153.
- Panek JA. 1996.** Correlations between stable carbon-isotope abundance and hydraulic conductivity in Douglas-fir across a climate gradient in Oregon, USA. *Tree Physiology* **16**, 747-755.

- Pitman GB, Hedden RL, Gara RI. 1975.** Synergistic effects of ethyl alcohol on the aggregation of *Dendroctonus pseudotsugae* (Coleoptera: Scolytidae) in response to pheromones. *Journal of Applied Entomology* **78**: 203-208.
- Pouttu A, Dobbertin M. 2000.** Needle-retention and density patterns in *Pinus sylvestris* in the Rhone Valley of Switzerland: comparing results of the needle-trace method with visual defoliation assessments. *Canadian Journal of Forest Research* **30**: 1973-1982.
- Puritch GS. 1971.** Water permeability of the wood of grand fir (*Abies grandis* (Dougl.) Lindl.) in relation to infestation by the balsam wooly aphid, *Adelges piceae* (Ratz.). *Journal of Experimental Botany* **22**: 936-945.
- Quick WP, Chaves MM, Wendler R, David M, Rodrigues ML, Passaharinho JA, Pereira JS, Adcock MD, Leegood RC, Stitt M. 1992.** The effect of water stress on photosynthetic carbon metabolism in four species grown under field conditions. *Plant, Cell & Environment* **15**: 25-35.
- Rabbinge R, Jorritsma ITM, Schans J. 1985.** Damage components of powdery mildew in winter wheat. *Netherlands Journal of Plant Pathology* **91**: 235-247.
- Rhode T. 1937.** Concerning the Swiss Douglas blight and its suspected cause *Adelopus* sp. *Mitteilungen aus Fortwirtschaft und Forstwissenschaft* **4**: 487-514. Translation of German manuscript from University of Michigan.
- Roden JS, Ehleringer JR. 1999.** Hydrogen and oxygen isotope ratios of tree-ring cellulose for riparian trees grown long-term under hydroponically controlled environments. *Oecologia* **121**: 467-477.
- Ross DW, Daterman GE. 1997.** Using pheromone-baited traps to control the amount and distribution of tree mortality during outbreaks of the Douglas-fir beetle. *Forest Science* **43**: 65-70.
- Rosso PH, Hansen EM. 2003.** Predicting Swiss needle cast distribution and severity in young Douglas-fir plantations in coastal Oregon. *Phytopathology* **93**: 790-798.
- Ryan MG. 2011.** Tree responses to drought. *Tree Physiology* **31**: 237-239.
- Sala A, Piper F, Hoch G. 2010.** Physiological mechanisms of drought-induced tree mortality are far from being resolved. *New Phytologist* **186**: 274-281.

- Sala A, Woodruff DR, Meinzer FC. 2012.** Carbon dynamics in trees: feast or famine? *Tree Physiology* **32**: 764-775.
- Schaberg PG, Snyder MC, Shane JB, Donnelly JR. 2000.** Seasonal patterns of carbohydrate reserves in red spruce seedlings. *Tree Physiology* **20**: 549-555.
- Seibt U, Wingate L, Berry JA, Lloyd J. 2006.** Non-steady state effects in diurnal ¹⁸O discrimination by *Picea sitchensis* branches in the field. *Plant, Cell & Environment* **29**: 928-939.
- Seibt U, Rajabi A, Griffiths H, Berry, JA. 2008.** Carbon isotopes and water use efficiency: sense and sensitivity. *Oecologia* **155**: 441-454.
- Secchi F, Zwieniecki MA. 2011.** Sensing embolism in xylem vessels: the role of sucrose as a trigger for refilling. *Plant, Cell & Environment* **34**: 514-524.
- Shaw DC, Filip GM, Kanaskie A, Maguire DA, Littke WA. 2011.** Managing an epidemic of Swiss Needle Cast in the Douglas-fir region of Oregon: the role of the Swiss Needle Cast Cooperative. *Journal of Forestry* **109**: 109-119.
- Silpi U, Lacoite A, Kasempap P, Thanysawanyangkura S, Chantuma P, Gohet E, Musigamart N, Clément A, Améglio T, Thaler P. 2007.** Carbohydrate reserves as a competing sink: evidence from tapping rubber trees. *Tree Physiology* **27**: 881-889.
- Simms HR. 1967.** On the ecology of *Herpotrichia nigra*. *Mycologia* **59**: 902-909.
- Sinclair W, Lyon HH. 2005.** *Diseases of trees and shrubs*. Ithaca, USA: Cornell University Press.
- Snyder KA, Monnar R, Poulson SR, Hartsough P, Biondi F. 2010.** Diurnal variations of needle water isotopic ratios in two pine species. *Trees* **24**: 585-595.
- Soderström B. 2002.** Challenges for mycorrhizal research into the new millennium. *Plant and Soil* **244**: 1-7.
- Song X, Barbour MM, Farquhar GD, Vann DR, Helliker BR. 2013.** Transpiration rate relates to within- and across-species variations in effective path length in a leaf water model of oxygen isotope enrichment. *Plant, Cell & Environment* **36**: 1338-1351.

- Srichuwong S, Jane JL. 2007.** Physicochemical properties of starch affected by molecular composition and structures: a review. *Food Science and Technology* **16**: 663–674.
- Sternberg LSL. 1989.** Oxygen and hydrogen isotope ratios in plant cellulose: mechanisms and applications. In: Rundel PW, Ehrlinger JR, Nagy KA, eds. *Stable Isotopes in Ecological Research*. Berlin, DE: Springer-Verlag, 124-141.
- Stone, JK. 1987.** Initiation and development of latent infections by *Rhabdocline parkerii* on Douglas-fir. *Canadian Journal of Botany* **65**: 2614-2621.
- Stone JK, Reeser PW, Kanaskie A. 2007.** Fungicidal suppression of Swiss needle cast and pathogen reinvasion in a 20-year-old Douglas-fir stand in Oregon. *Western Journal of Applied Forestry* **22**: 248-252.
- Stone JK, Capitano BR, Kerrigan JL. 2008a.** The histopathology of *Phaeocryptopus gaeumannii* on Douglas-fir needles. *Mycologia* **11**: 431-444.
- Stone JK, Coop LB, Danter DK. 2008b.** Predicting effects of climate change on Swiss needle cast disease severity in Pacific Northwest forests. *Canadian Journal of Plant Pathology* **30**: 169-176.
- Sveinbjornsson B, Smith M, Traustason T, Ruess RW, Sullivan PF. 2010.** Variation in carbohydrate source-sink relations of forest and treeline white spruce in southern, interior and northern Alaska. *Oecologia* **163**: 833-843.
- Tainter FH, Baker FA. 1996.** *Principles of forest pathology*. Hoboken, USA: John Wiley & Sons, Inc.
- Trappe JM, Strand RF. 1969.** Mycorrhizal deficiency in a Douglas-fir region nursery. *Forest Science* **15**: 381-389.
- Turgeon R. 2010.** The role of phloem loading reconsidered. *American Society of Plant Biologists* **152**: 1817-1823.
- Wang XF, Yakir D. 1995.** Temporal and spatial variations in the oxygen-18 content of leaf water in different plant species. *Plant, Cell & Environment* **18**: 1377-1385.
- Wang Z, Stutte GW. 1992.** The role of carbohydrates in active osmotic adjustment in apple under water stress. *Journal of the American Society for Horticultural Science* **117**: 816-823.

- Warren CR, Adams MA. 2000.** Water availability and branch length determine $\delta^{13}\text{C}$ in foliage of *Pinus pinaster*. *Tree Physiology* **20**: 637-643.
- Warren CR, Ethier GJ, Livingston NJ, Grant NJ, Turpin DH, Harrison DL, Black TA. 2003.** Transfer conductance in second growth Douglas-fir (*Pseudotsuga menziesii* (Mirb.) Franco) canopies. *Plant, Cell & Environment* **26**: 1215-1227.
- Warton DI, Wright IJ, Falster DS, Westoby M. 2006.** Bivariate line-fitting methods for allometry. *Biological Reviews* **81**: 259-291.
- Webb WL. 1981.** Relation of starch content to conifer mortality and growth loss after defoliation by the Douglas-fir tussock moth. *Forest Science* **27**: 224-232.
- Webb WL, Karchesy JJ. 1977.** Starch content of Douglas-fir defoliated by the tussock moth. *Canadian Journal of Forest Research* **7**: 186-188.
- Weiskittel AR, Maguire DA, Garber SM, Kanaskie A. 2006.** Influence of Swiss needle cast on foliage age-class structure and vertical foliage distribution in Douglas-fir plantations in north coastal Oregon. *Canadian Journal of Forest Research* **36**: 1497-1508.
- Wiley E, Helliker B. 2012.** A re-evaluation of carbon storage in trees lends greater support to carbon limitation to growth. *New Phytologist* **195**: 285-289.
- Woodruff DR, Meinzer FC. 2011a.** Water stress, shoot growth and storage of non-structural carbohydrates along a tree height gradient in a tall conifer. *Plant, Cell & Environment* **34**: 1920-1930.
- Woodruff DR, Meinzer FC. 2011b.** Size-dependent changes in biophysical control of tree growth: the role of turgor. In: Meinzer FC, Lachenbruch B, Dawson T, eds. *Size- and Age-Related Changes in Tree Structure and Function*. Dordrecht, NL: Springer, 363-384.
- Würth MKR, Pelaez-Riedl S, Wright SJ, Körner C. 2005.** Non-structural carbohydrate pools in a tropical forest. *Oecologia* **143**: 11-24.
- Xiao Y. 2003.** Variation in needle longevity of *Pinus tabulaeformis* forests at different geographic scales. *Tree Physiology* **23**: 463-471.
- Yakir D, DeNiro MJ. 1990.** Oxygen and hydrogen isotope fractionation during cellulose metabolism in *Lemma gibba* L. *Plant Physiology* **93**: 325-332.

Zhao J, Maguire DA, Mainwaring DB, Kanaskie A. 2011. Climatic influences on needle cohort survival mediated by Swiss needle cast in coast Douglas-fir. *Trees* **26**: 1361-1371.

Appendix

Appendix A- Chapter 3 Supporting Information

Table A.1 Average total non-structural carbohydrate, starch, sucrose, and glucose and fructose concentrations (% dry weight) of twigs and foliage from 2011, 2010, and 2009 cohorts of Douglas-fir trees with Swiss Needle Cast sampled in mid-June.

Tree ID	Twig NSC (%)			Twig starch (%)			Twig sucrose (%)			Twig gluc/fruc (%)			Foliage NSC (%)			Foliage starch (%)			Foliage sucrose (%)			Foliage gluc/fruc (%)		
	2011	2010	2009	2011	2010	2009	2011	2010	2009	2011	2010	2009	2011	2010	2009	2011	2010	2009	2011	2010	2009	2011	2010	2009
1	5.59	3.50	2.44	3.96	2.29	1.67	0.70	0.66	0.43	0.92	0.55	0.35	4.02	2.72	-	0.70	0.95	-	1.85	0.99	-	1.47	0.79	-
2	7.49	5.40	4.20	5.61	3.62	2.90	0.87	1.03	0.64	1.01	0.75	0.66	9.48	5.11	4.01	5.49	2.11	1.46	2.36	2.09	1.84	1.63	0.91	0.71
3	5.95	3.50	2.53	3.78	2.29	1.74	0.50	0.49	0.36	1.68	0.72	0.43	5.60	3.78	-	2.52	1.71	-	1.28	0.89	-	1.80	1.19	-
4	5.58	5.13	4.10	2.73	3.53	2.92	1.31	0.79	0.74	1.54	0.82	0.44	10.08	5.71	5.70	6.48	3.09	3.49	2.08	1.56	1.78	1.52	1.06	0.43
5	2.74	2.80	2.31	1.60	1.59	1.47	0.58	0.64	0.40	0.55	0.56	0.44	7.08	4.42	-	2.55	1.27	-	2.74	1.92	-	1.80	1.23	-
6	7.30	6.31	5.53	4.18	3.80	3.14	1.20	0.90	0.95	1.92	1.61	1.44	5.61	3.72	-	2.23	1.39	-	2.17	1.47	-	1.22	0.85	-
7	3.97	3.10	2.53	1.80	1.20	0.91	0.37	0.44	0.37	1.80	1.45	1.25	7.67	3.40	-	4.20	1.45	-	1.25	1.06	-	2.21	0.89	-
8	6.58	3.60	-	4.54	2.24	-	1.09	0.63	-	0.95	0.73	-	7.55	3.02	-	3.78	1.03	-	2.14	1.23	-	1.64	0.76	-
9	7.20	5.12	3.93	4.55	3.32	2.67	1.21	1.03	0.64	1.45	0.77	0.61	6.01	2.18	-	2.80	0.70	-	2.26	0.69	-	0.94	0.78	-
10	6.06	4.99	4.47	3.81	2.61	2.20	0.43	0.65	0.29	1.82	1.73	1.98	6.10	4.87	-	2.80	2.29	-	1.47	1.47	-	1.83	1.12	-
11	6.84	4.57	3.83	4.69	3.02	2.61	1.03	0.82	0.72	1.11	0.73	0.50	7.85	6.74	-	3.50	3.64	-	2.56	1.76	-	1.79	1.34	-
12	8.11	4.58	3.38	5.92	3.21	2.49	1.07	0.83	0.57	1.11	0.54	0.32	8.47	4.92	-	4.56	2.55	-	2.12	1.62	-	1.79	0.75	-
13	7.37	3.89	2.59	5.43	2.44	1.41	1.00	0.83	0.67	0.93	0.61	0.51	4.74	-	-	1.38	-	-	1.68	-	-	1.68	-	-
14	4.40	2.69	2.79	2.12	1.10	1.45	1.13	0.85	0.68	1.15	0.74	0.66	3.54	1.49	-	1.25	0.55	-	1.07	0.55	-	1.21	0.40	-
15	6.49	2.82	2.88	4.41	1.58	1.94	1.19	0.74	0.69	0.89	0.50	0.26	3.39	3.05	-	0.87	0.83	-	1.72	1.48	-	0.81	0.74	-

Table A.2 Average total non-structural carbohydrate, starch, sucrose, and glucose and fructose concentrations (% dry weight) of twigs and foliage from 2011, 2010, and 2009 cohorts of Douglas-fir trees with Swiss Needle Cast sampled in late July.

Tree ID	Twig NSC (%)			Twig starch (%)			Twig sucrose (%)			Twig gluc/fruc (%)			Foliage NSC (%)			Foliage starch (%)			Foliage sucrose (%)			Foliage gluc/fruc (%)		
	2011	2010	2009	2011	2010	2009	2011	2010	2009	2011	2010	2009	2011	2010	2009	2011	2010	2009	2011	2010	2009	2011	2010	2009
1	3.20	2.60	2.25	1.10	1.07	1.14	1.00	0.93	0.51	1.10	0.60	0.60	4.64	3.26	-	0.70	0.53	-	1.98	1.58	-	1.96	1.16	-
2	4.85	3.44	2.32	1.81	1.35	0.81	1.30	0.93	0.79	1.75	1.16	0.72	7.16	5.20	-	1.99	1.11	-	2.46	2.42	-	2.72	1.67	-
3	3.34	3.21	1.91	0.21	0.62	0.31	1.44	1.37	0.86	1.69	1.21	0.75	3.78	3.75	-	0.36	0.87	-	1.69	1.04	-	1.74	1.84	-
4	6.50	4.29	3.52	1.41	0.85	0.84	2.09	1.76	1.31	3.00	1.69	1.37	5.36	4.16	3.35	0.61	0.50	0.42	2.61	2.33	2.01	2.15	1.33	0.92
5	4.62	3.23	2.75	0.93	0.70	0.71	1.36	1.11	0.79	2.33	1.41	1.25	6.49	3.45	-	1.87	0.59	-	2.22	1.87	-	2.40	0.99	-
6	6.03	4.69	4.17	1.21	1.52	1.94	2.53	1.85	1.32	2.30	1.33	0.90	6.22	5.13	-	1.77	1.53	-	2.36	2.26	-	2.09	1.34	-
7	5.11	3.68	2.59	0.54	0.28	0.24	1.33	1.91	0.71	3.25	1.49	1.64	7.00	5.94	-	2.16	2.18	-	2.46	2.49	-	2.38	1.27	-
8	4.83	3.47	3.27	1.45	1.23	1.68	1.39	1.01	0.73	1.99	1.23	0.86	4.02	3.16	-	0.88	0.73	-	1.51	1.14	-	1.63	1.30	-
9	5.44	3.88	2.73	2.12	1.33	1.53	1.55	1.26	0.60	1.77	1.29	0.60	4.66	2.35	-	0.54	0.44	-	2.41	1.10	-	1.72	0.81	-
10	6.85	5.21	4.17	2.85	2.56	1.90	0.85	0.49	0.46	3.15	2.15	1.81	6.75	5.57	-	2.20	1.80	-	1.70	1.28	-	2.85	2.49	-
11	6.41	6.11	4.85	1.93	2.57	2.46	1.22	1.40	1.26	3.26	2.13	1.13	4.92	4.71	-	0.82	0.69	-	1.85	2.07	-	2.25	1.96	-
12	4.55	3.36	2.19	2.07	1.23	0.68	1.24	1.21	0.77	1.24	0.92	0.73	5.31	4.17	3.74	1.00	0.67	0.85	2.28	2.21	1.67	2.03	1.29	1.22
13	3.59	2.93	2.36	1.45	1.39	1.35	1.19	0.99	0.56	0.95	0.55	0.45	3.86	3.84	-	0.55	0.57	-	1.87	1.90	-	1.44	1.37	-
14	4.02	2.06	2.12	0.90	0.36	0.78	0.77	0.79	0.68	2.36	0.91	0.67	5.31	2.82	-	1.24	0.73	-	2.00	1.27	-	2.07	0.82	-
15	2.45	1.71	1.54	0.15	0.08	0.13	1.03	0.87	0.60	1.27	0.76	0.81	4.30	2.78	-	0.47	0.57	-	2.23	1.20	-	1.61	1.01	-

Table A.3 Average total non-structural carbohydrate, starch, sucrose, and glucose and fructose concentrations (% dry weight) of twigs and foliage from 2011, 2010, and 2009 cohorts of Douglas-fir trees with Swiss Needle Cast sampled in early September.

Tree ID	Twig NSC			Twig starch			Twig sucrose			Twig gluc/fruc			Foliage NSC			Foliage starch			Foliage sucrose			Foliage gluc/fruc		
	2011	2010	2009	2011	2010	2009	2011	2010	2009	2011	2010	2009	2011	2010	2009	2011	2010	2009	2011	2010	2009	2011	2010	2009
1	2.05	1.66	1.07	0.48	0.25	0.27	0.57	0.66	0.40	1.01	0.76	0.40	4.20	2.70	-	0.70	0.61	-	1.82	1.10	-	1.68	0.99	-
2	6.96	4.96	3.48	3.19	1.96	1.07	1.89	1.42	1.23	1.87	1.59	1.17	6.60	4.30	3.97	1.29	0.61	0.57	3.04	2.40	2.29	2.27	1.29	1.11
3	2.72	2.51	1.57	0.22	0.41	0.37	0.63	0.73	0.43	1.88	1.37	0.77	3.08	3.05	-	0.48	1.05	-	1.44	0.78	-	1.15	1.22	-
4	2.86	1.94	1.58	0.62	0.29	0.34	0.90	0.62	0.55	1.35	1.03	0.68	5.41	4.49	3.51	0.86	0.70	0.64	2.57	2.34	1.83	1.98	1.45	1.05
5	2.09	1.31	0.73	0.39	0.23	0.16	0.77	0.51	0.37	0.93	0.57	0.20	5.96	3.75	-	1.34	0.77	-	2.64	1.87	-	1.98	1.11	-
6	2.57	2.34	1.43	0.37	0.53	0.36	1.27	1.08	0.70	0.93	0.73	0.36	3.93	3.77	-	0.25	0.54	-	2.64	2.32	-	1.05	0.91	-
7	3.27	2.25	1.60	0.51	0.47	0.21	1.43	0.74	0.67	1.34	1.03	0.71	3.66	2.65	-	0.43	0.23	-	2.25	2.01	-	0.98	0.41	-
8	3.57	2.55	2.01	0.65	0.73	0.47	1.13	0.82	0.82	1.79	1.00	0.72	3.91	3.72	-	0.45	0.31	-	2.03	2.10	-	1.43	1.31	-
9	3.43	2.26	1.40	0.35	0.34	0.47	1.39	0.92	0.51	1.68	1.00	0.42	3.65	2.58	-	0.33	0.62	-	2.15	1.04	-	1.17	0.93	-
10	4.31	3.67	2.63	0.65	0.76	0.60	1.83	1.56	1.06	1.82	1.35	0.97	5.03	3.88	-	0.21	0.32	-	3.42	2.54	-	1.41	1.02	-
11	4.59	4.34	3.42	1.04	1.54	1.77	1.90	1.54	1.05	1.66	1.26	0.60	4.85	4.62	3.06	0.52	0.45	0.42	2.65	2.83	1.88	1.68	1.34	0.76
12	3.47	2.59	1.92	0.72	0.35	0.35	1.45	1.14	0.47	1.30	1.09	1.09	4.41	3.43	2.56	0.37	0.28	0.37	2.61	2.23	1.51	1.43	0.92	0.68
13	2.36	1.55	1.16	0.65	0.52	0.38	0.88	0.54	0.44	0.83	0.49	0.34	3.06	-	-	0.45	-	-	1.49	-	-	1.12	-	-
14	2.06	1.11	0.92	0.61	0.34	0.22	0.69	0.42	0.33	0.76	0.36	0.37	4.74	3.31	-	0.58	0.13	-	2.09	2.19	-	2.07	1.00	-
15	2.06	1.18	1.00	0.20	0.09	0.10	0.87	0.53	0.41	0.98	0.57	0.50	4.30	2.98	-	0.01	0.14	-	2.76	2.00	-	1.71	0.87	-

